UC Irvine
UC Irvine Electronic Theses and Dissertations

Title

Development of Protein Microarray Fabrication Methods for Analysis by Surface Plasmon Resonance Imaging

Permalink

https://escholarship.org/uc/item/5hb0k3jr

Author

Manuel, Gerald Paulo

Publication Date

2017

Copyright Information

Peer reviewed|Thesis/dissertation

UNIVERSITY OF CALIFORNIA,
IRVINE

Development of Protein Microarray Fabrication Methods for Analysis
by Surface Plasmon Resonance Imaging

DISSERTATION

submitted in partial satisfaction of the requirements
for the degree of

DOCTOR OF PHILOSOPHY

in Chemistry

by

Gerald Paulo Manuel

Dissertation Committee:
Professor Robert M. Corn, Chair
Professor Andrej Lupták
Professor Gregory A. Weiss

2017

DEDICATION

To my mother, Maria, my father, Gil, and my Uncle Jun.

TABLE OF CONTENTS

LIST OF FIGURES

LIST OF TABLES

LIST OF SYMBOLS

θ: Angle from normal incidence for SPRI reflectivity.

λ: Wavelength

Δ%R: Change in percent reflectivity

Acknowledgments

As my graduate career comes to a close and I begin to reflect on my 5 years here at UCI, I realize how fortunate I am to have the unwavering support of my family, friends, and colleagues. These relationships are the foundation of my dissertation. From the bottom of my heart, thank you all so much. I couldn't have done it without you.

First and foremost, I would like to thank my advisors Rob Corn and Andrej Lupták. Rob, thank you for your patience and your guidance. Thank you for your constant optimism when the science wasn't going so well and your enthusiasm when the results were flowing. Andrej, thank you for your unending stream of ideas and your willingness to personally teach me how to use basically any machine in either of our labs.

To my fiancé Lindsay, thank you for you love and support, and for being my confidant and my best friend. Thanks for making me go to the beach after orals and for making me comfort food or taking me out to a bar after a bad lab day. None of this is possible without your day-to-day support.

To my parents, Gil and Maria, thank you for raising me to be scientifically curious and for teaching me how to work hard, particularly when I don't feel like it. The traits you instilled in me during my youth are critical to my success today. Thank you for all the sacrifices you've made raising my sisters and I. You did an amazing job with the three of us. To my sisters Steph and KK, thanks for answering my random FaceTime calls and for the revitalizing breaks in Fresno. Thanks for making sure we always got Me N Eds and Doghouse and for simply making home feel like home. To my Uncle Jun, thank you for sharing your knowledge about your graduate school experience and for cultivating my curiosity for science in my youth. Your guidance has been indispensible. This dissertation is a direct result of your influence.

To former and current group members, thank you for keeping daily life in the Corn lab light and fun. I feel incredibly fortunate to have joined a research group full of passionate scientists and lifelong friends. To Mike and Jenn, thank you for your mentorship throughout my graduate career. Mike, thanks for teaching me the fundamentals of SPRI and for the ping pong breaks. Jenn, thanks for letting me vent to you about science and for exploring all the food in Orange County with me. To the CGGC, some of my best memories were competing with all of you. I hope you finish off our list, particularly the escape room. To Adam, Millie, and Kellen, thank you for convincing me to go to Disneyland all those times. I needed it. To Anna, the zinc finger project wouldn't be where it is without you. Thanks for being such a bubbly, positive presence in our office. Your ability to find the good in basically any situation was refreshing at a time in my career when I was pretty pessimistic about science. I'll miss our morning coffee runs and our walks after subgroup.

To my friends, Sam, Hannah, Alana, Will, Andrew, and Andrea, thanks for being my weekend escapes from lab. Hanging out with you guys was often the highlight of my week. I'll miss our rage cage dates, going to beer fests, and hanging out by the pool. I'll never forget that duffy boat in Newport and our shenanigans in San Diego. Patrón, tequila.

Lastly, to all my intramural teams, Sharks with Lasers, Bad Life Choices, and Real Men Love Pluots, thank you all for providing me a physical, competitive outlet during my time at UCI. I had the time of my life winning and losing with you, finding hatred for various teams (looking at you squishy ball), and cracking jokes at the expense unfortunate plays/players.

This dissertation belongs to all of you as much as it does to me. I hope you find the work presented in this dissertation informative and inspiring.

CURRICULUM VITAE

Gerald P. Manuel
gerald.manuel18@gmail.com

Education

Ph.D., Chemistry, University of California, Irvine (Irvine, CA) 2017
Dissertation: Development of Protein Microarrays for Analysis by Surface Plasmon Resonance Imaging
Advisor: Professor Robert M. Corn

B.S., Biochemistry, University of California, Riverside (Riverside, CA) 2012
Undergraduate Research Project: Synthesis of Phosphorous Containing N-Heterocyclic Carbenes
Advisor: Professor Guy Bertrand

Professional Experience

Graduate Student Researcher, Chemistry
Department of Chemistry University of California, Irvine, 2012-2017

Undergraduate Researcher, Chemistry Department of Chemistry University of California, Riverside, 2008-2012

Laboratory Technician
BSK Laboratories, Fresno, CA 2007-2009

Research Publications:

Chen, J., Manuel, G., Corn, M. R., Luptàk, A., & Golden, B. L. (2017). Engineering a ribozyme with tRNA synthetase activity. *Submitted.*

Gerald Manuel, Andrej Luptàk, and Robert M. Corn, "A Microwell-Printing Fabrication Strategy for the On-Chip Templated Biosynthesis of Protein Microarrays for Surface Plasmon Resonance Imaging" *J. Phys. Chem. C,* **120** ASAP article (2016)

Ryan Spencer, Kevin H. Chen, Gerald Manuel, and James S. Nowick, "Recipe for β-Sheets: Foldamers Containing Amyloidogenic Peptide Sequences" *Eur. J. Org. Chem.* **17**, 3523-3528 (2013)

David Martin, Nicolas Lassauque, Florian Steinmann, Gerald Manuel, and Guy Bertrand, "Experimental and Computational Studies of Anti-Bredt Amidinium Salts" *Chem. Eur. J.* **44**, 14895- 14901

Awards and Presentations

University of California Drug Discovery Consortium Fellowship, 2017

American Chemical Society National Conference – San Diego, 2016

Pacifichem Student Poster Competition, Finalist, 2015

New England Biolabs Poster Award, RNA Society, 2015

Dean's Undergraduate Research Fellowship. 2008

ABSTRACT OF THE DISSERTATION

Development of Protein Microarray Fabrication Methods for Analysis by Surface Plasmon
Resonance Imaging

By

Gerald Manuel

Doctor of Philosophy in Chemistry

University of California, Irvine, 2017

Professor Robert Corn, Chair

This dissertation is the culmination of work toward the development of protein microarrays for surface plasmon resonance imaging (SPRI). Two main issues with protein microarrays for SPRI are addressed. First, we will address issues with introducing spatial selectivity into protein microarray fabrication strategies. We solve this problem first by physical separation of protein synthesis in a microwell array, followed by contact printing onto a functionalized SPRI chip. In our second solution for this spatial selectivity problem, we introduce a novel protein adsorption chemistry based on zinc finger/DNA affinity. This chemistry is explored as a potential adsorption chemistry for self-assembled protein microarrays.

The second issue we will address is lack of unnatural amino acids in current protein microarray fabrication methods. Unnatural amino acids allow users to introduce precise chemical control into proteins, but despite their utility, they have not been introduced into current fabrication strategies because of their biosynthetic difficulty. We address this issue by introducing an on chip amber suppression strategy, using a ribozyme based tRNA misacylation system.

Chapter 1

Introduction

1.1 Dissertation Overview

Protein microarrays have become powerful tools for the high-throughput study of proteins and their functions.[1–3] Coupled with genomic sequencing, these arrays have enabled genome-wide screens for protein/protein interactions, expanding our knowledge of whole proteomes. A majority of these arrays use fluorescently tagged proteins to visualize specific adsorption to arrayed targets.[2] However, there are drawbacks to using fluorescence based detection methods: first, labeling proteins with small molecule fluorophores is difficult and requires numerous purification and synthesis steps that are often cost prohibitive at large scale.[4] Further, labeling proteins in this manner may perturb natural protein/protein interactions resulting in both false positive and false negative results. Surface Plasmon Resonance Imaging (SPRI), in contrast, circumvents the issues outlined above because it is a method that relies on changes in the refractive index of a gold thin-film surface to detect surface adsorption events, allowing SPRI to be *label-free* bioaffinity sensing technique.[5–7] Despite this advantage, few protein microarrays suitable for high-throughput analysis by SPRI have been reported.[8]

This dissertation is the culmination of work toward the development of protein microarrays suitable for SPRI. In Chapter 2, we will discuss the fabrication of protein microarrays using a microwell-based contact printing method. Next, a method using zinc-finger fusion proteins for the self-assembly of protein microarrays will be described in Chapter 3. Finally, the last chapter of this dissertation will focus on the introduction of recoded protein microarrays as a step toward the creation of unnatural protein microarrays via amber suppression technology.

1.2 Surface Plasmon Resonance Imaging[7]

SPRI is a label free, surface sensitive technique used throughout this dissertation for the detection of protein adsorption to chemically modified surfaces. SPRI is driven by surface plasmon polaritons (SPPs), which are electromagnetic waves that propagate along a thin-film metal/dielectric interface. At specific resonance conditions, photons excite SPPs by the coupling of photons to the plasmons of the metal surface. In our work, wave vector matched, p-polarized light fulfills these resonance conditions in a geometry known as the Kretschmann configuration. As shown in Figure 1.1, collimated 800 nm light passes through a polarizer before encountering a high refractive index prism and reflecting off the back of a gold thin film surface. At the SPR angle, θ_{SPR}, the resonance conditions are met causing the light at θ_{SPR} to be converted into SPPs, resulting in a reflectivity decrease as illustrated in the reflectivity curve as shown in Figure 1.2. SPP intensity decays exponentially with increasing distance from the surface, with a decay length of only a few hundred nanometers, meaning SPR is highly sensitive to surface perturbation. Upon a change in the refractive index in response to surface adsorption, the SPP resonance conditions change, causing a shift in the reflectivity curve (red to blue in Figure 1.2) and in θ_{SPR}. Commonly, the change in θ_{SPR} is measured, however in SPRI, the change in percent reflectivity ($\Delta\%R$) is measured at a fixed angle, termed the SPRI angle (θ_{SPRI}), as surface adsorption events occur. Measuring reflectivity at a fixed angle (θ_{SPRI}) as opposed to measuring θ_{SPR} enhances experimental sensitivity by monitoring changes at the steepest part of the reflectivity curve while also enabling the observation of whole microarrays simultaneously.
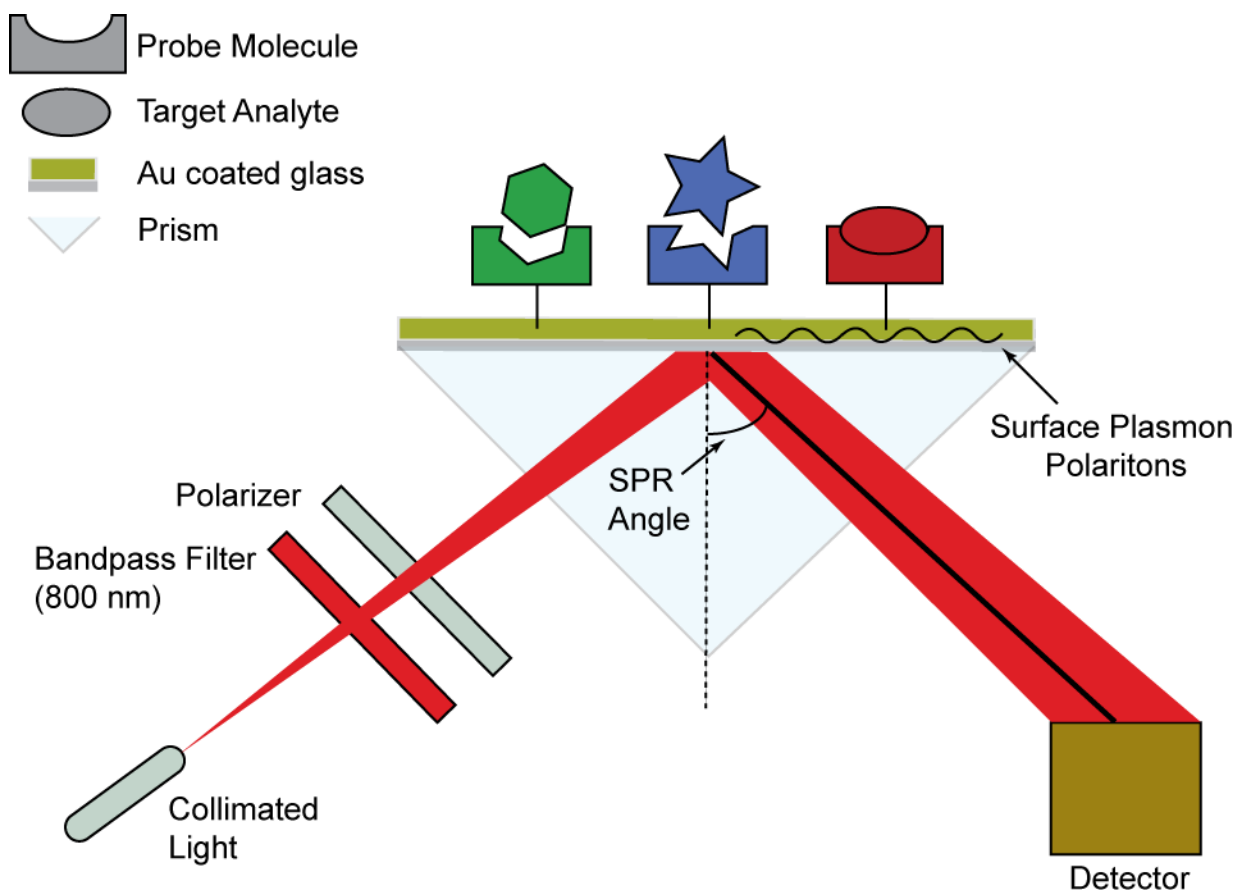
Figure 1.1: Surface Plasmon Resonance Imaging. Collimated, p-polarized light is reflected off the back of a gold thin film surface and captured by a detector (in this case a CCD camera). At the SPR angle, this light is absorbed to create surface plasmon polaritons. Adsorption of analytes to the surface causes a change in the SPR angle, providing a medium for detection.

1.3 Microwell-Printing Fabrication Strategy for Protein Microarrays Suitable for SPRI[9]

Our research group's first attempt at creating protein microarrays for SPRI was performed by Dr. Ting Seefeld.[10] In this work, protein microarrays were synthesized on-chip by introducing an in-vitro transcription/translation (IVTT) reaction solution via microfluidics to a protein encoding dsDNA array. After on-chip synthesis, His$_6$-tagged proteins were captured by adjacent Cu^{II}-nitrilotriacetic acid (NTA) capture elements and then confirmed by antibody
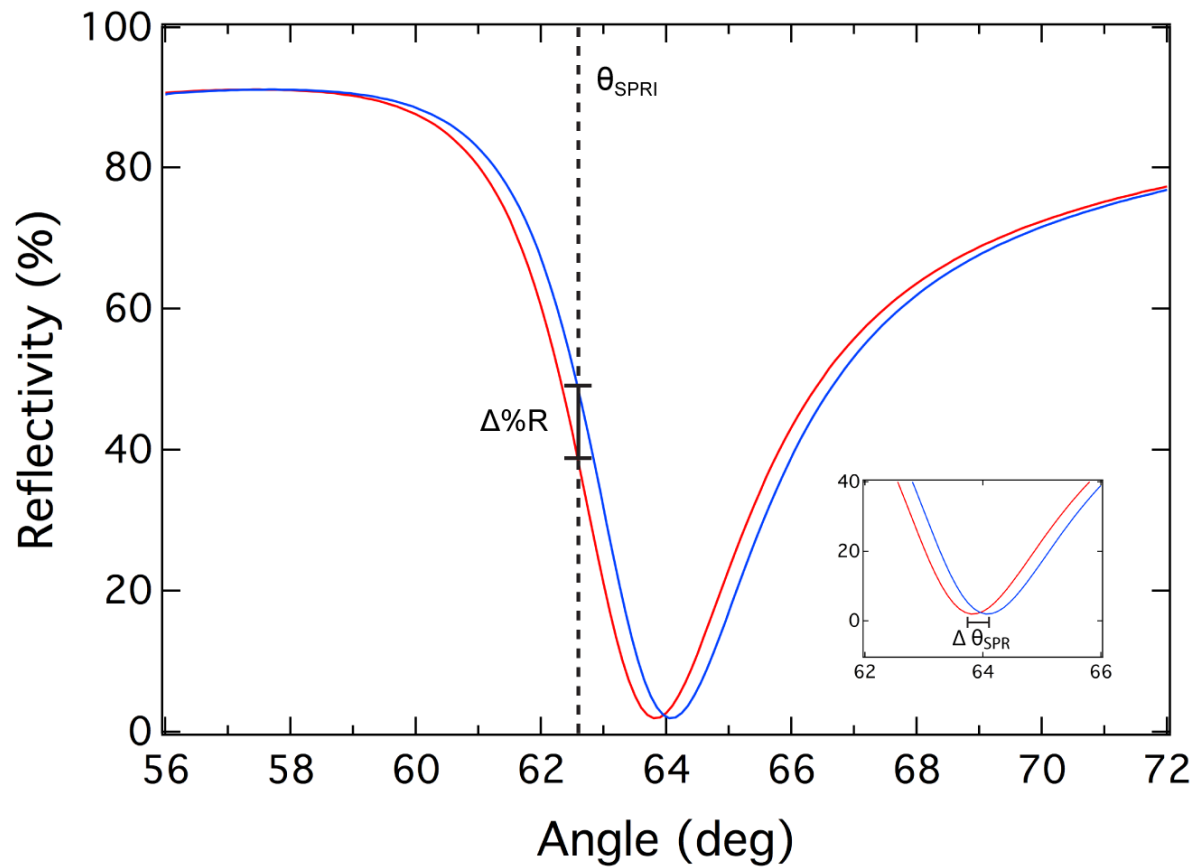
Figure 1.2: SPR Reflectivity Curve. At the SPR angle, light is absorbed to generate surface plasmon polaritons, resulting in a % reflectivity decrease. In SPRI, the change in reflectivity $\Delta\%R$ is measured.

adsorption. This work provided important breakthroughs for SPRI based protein microarrays, though practical shortcomings prevented this method from becoming a viable protein microarray fabrication technique. The overarching limitation of this technique is the small number of proteins that can be arrayed on a single SPRI chip. The use of a universal capture tag (His$_6$-tag), coupled with microfluidics used to deliver the IVTT solutions to the array, limits this technique to only one protein per microfluidic channel.

In Chapter 2, we attempt to solve this one protein/one channel problem by creating a new protein microarray fabrication method: Microwell-Printing Fabrication Strategy for Protein Microarrays Suitable for SPRI.[9] In this method, His$_6$-tagged proteins were synthesized in a 16-component, 4 x 4, polyolefin microwell array followed by contact printing onto a nitrilotriacetic acid (NTA) functionalized SPRI chip for His$_6$-tag protein capture on chip. This immobilized protein array was then used in detecting protein/protein interactions by SPRI. This microwell array facilitates physical separation during protein synthesis to drive spatial selectivity of the protein microarray on the SPRI chip, avoiding the one protein/one channel issue encountered by Seefeld *et al*. Using this method, we created a 3-component protein microarray with GFP, YFP, and mCherry and then used this array to detect antibody adsorption. Compared to our group's previous microfluidic based biosynthesis method, this microwell based method exhibited a 50-fold increase in sensitivity. In addition to this increase in sensitivity, we were able to examine protein mixtures for affinity to these protein arrays. We found that while monoclonal anti-GFP adsorbed specifically to GFP elements as expected, a polyclonal anti-GFP mixture adsorbed to both GFP and YFP revealing the proportion of GFP and YFP binding antibodies present in the mixture. Finally, antibodies specific for mCherry adsorbed specifically to mCherry elements despite the same β-barrel tertiary structure as GFP and YFP.

Despite these improvements upon our previous protein array fabrication methods, this method and many others suffer from the use of a single, universal capture chemistry *i.e.* each protein in the array carries the same capture tag. The use of universal capture tags limits researchers to physically separating proteins, via microwells or spotting, to implement spatial selectivity within microarrays. To move away from physical separation, we aimed to create a chemistry that captures proteins with spatial selectivity. These capture chemistries need to be unique for each protein and orthogonal to one another. Unfortunately, not enough bioorthogonal chemistries exist to create even a 16-element protein microarray. We turned to biology for inspiration to create a large number of capture chemistries, resulting in a zinc-finger mediated capture chemistry, which is described in Chapter 3 of this dissertation.

1.4 Zinc-Finger Mediated Self-Assembled Protein Microarrays

In order to create a large protein microarray suitable for a microfluidic format, a novel protein capture chemistry was developed. Taking inspiration from biology, we implemented the use of zinc-fingers (ZFs), which are proteins found in eukaryotes that bind to DNA with sequence specificity. ZFs are capable of binding a 3 base pair (bp) DNA sequence, and can be tethered together to bind longer DNAs.[11] The ability of ZFs to distinguish DNAs of different sequences coupled with our ability to form DNA surfaces for SPRI serves as an attractive platform to create self-assembled protein microarrays. In Chapter 3, we describe the fabrication of ZF mediated self-assembled protein microarrays. We first design and synthesize ZF-fusion proteins (ZFPs) consisting of ZFs fused to protein domains. We then show that these fusion proteins have functional ZF domains as well as functional tethered protein domains, and then show that these functions are not mutually exclusive by fluorescence microscopy. Following this

confirmation, we show that these proteins can recognize their DNAs on chip from a crude *in vitro* transcription/translation reaction solution.

1.5 Recoded Protein Microarrays via Amber Suppression

Proteins containing non-canonical amino acids (unnatural proteins) have found many practical uses as therapeutics, bioorthogonal chemical handles, and as probes for protein function.[12–14] Despite this broad use of unnatural proteins in various disciplines, unnatural proteins have yet to be included into existing protein microarray fabrication strategies due to their difficulty to produce.[15] Chapter 4 of this dissertation will outline our strategy for the incorporation of unnatural proteins into protein microarrays by an on-chip amber suppression strategy. This strategy is built upon the microwell-printing fabrication strategy described in Chapter 2. In this format, unnatural protein microwell arrays will be produced, however the unnatural amino acid incorporated in each microwell will be dictated by the misacylated tRNA added. tRNAs will be misacylated using a ribozyme based misacylation system developed by Suga *et. al.*[16] In this chapter, we provide a preliminary example of amber suppression in a microwell array, followed by contact printing onto an NTA-functionalized SPRI chip. Successful recoding of YFP by on chip amber suppression is shown by fluorescence microscopy. We then tested the fidelity of this "recoded" protein microarray by antibody analysis. SPRI of antibody adsorption to this recoded protein microarray confirms the synthesis of the recoded protein.

1.6 References

(1)   Duarte, J. G.; Blackburn, J. M. Advances in the Development of Human Protein Microarrays. *Expert Rev. Proteomics* **2017**, *14* (7), 627–641.

(2)   Moore, C. D.; Ajala, O. Z.; Zhu, H. Applications in High-Content Functional Protein Microarrays. *Curr. Opin. Chem. Biol.* **2016**, *30* (Supplement C), 21–27.

(3)   Hall, D. A.; Ptacek, J.; Snyder, M. Protein Microarray Technology. *Mech. Ageing Dev.* **2007**, *128* (1), 161–167.

(4)   Schumacher, D.; Hackenberger, C. P. More than Add-on: Chemoselective Reactions for the Synthesis of Functional Peptides and Proteins. *Curr. Opin. Chem. Biol.* **2014**, *22* (Supplement C), 62–69.

(5)   Singh, P. SPR Biosensors: Historical Perspectives and Current Challenges. *Sens. Actuators B Chem.* **2016**, *229*, 110–130.

(6)   Spoto, G.; Minunni, M. Surface Plasmon Resonance Imaging: What Next? *J. Phys. Chem. Lett.* **2012**, *3* (18), 2682–2691.

(7)   Smith, E. A.; Corn, R. M. Surface Plasmon Resonance Imaging as a Tool to Monitor Biomolecular Interactions in an Array Based Format. *Appl. Spectrosc.* **2003**, *57* (11), 320A–332A.

(8)   Kamat, V.; Rafique, A. Extending the Throughput of Biacore 4000 Biosensor to Accelerate Kinetic Analysis of Antibody-Antigen Interaction. *Anal. Biochem.* **2017**, *530* (Supplement C), 75–86.

(9)   Manuel, G.; Lupták, A.; Corn, R. M. A Microwell–Printing Fabrication Strategy for the On-Chip Templated Biosynthesis of Protein Microarrays for Surface Plasmon Resonance Imaging. *J. Phys. Chem. C* **2016**.

(10)   Seefeld, T. H.; Halpern, A. R.; Corn, R. M. On-Chip Synthesis of Protein Microarrays

from DNA Microarrays via Coupled In Vitro Transcription and Translation for Surface

Plasmon Resonance Imaging Biosensor Applications. *J. Am. Chem. Soc.* **2012**, *134* (30),

12358–12361.

(11)   Persikov, A. V.; Wetzel, J. L.; Rowland, E. F.; Oakes, B. L.; Xu, D. J.; Singh, M.; Noyes,

M. B. A Systematic Survey of the Cys2His2 Zinc Finger DNA-Binding Landscape.

Nucleic Acids Res. **2015**, *43* (3), 1965–1984.

(12)   Schneider, A. F. L.; Hackenberger, C. P. R. Fluorescent Labelling in Living Cells. *Curr.*

Opin. Biotechnol. **2017**, *48* (Supplement C), 61–68.

(13)   Blaskovich, M. A. T. Unusual Amino Acids in Medicinal Chemistry. *J. Med. Chem.* **2016**,

59 (24), 10807–10836.

(14)   Si, L.; Xu, H.; Zhou, X.; Zhang, Z.; Tian, Z.; Wang, Y.; Wu, Y.; Zhang, B.; Niu, Z.;

Zhang, C.; et al. Generation of Influenza A Viruses as Live but Replication-Incompetent

Virus Vaccines. *Science* **2016**, *354* (6316), 1170–1173.

(15)   Liu, C. C.; Schultz, P. G. Adding New Chemistries to the Genetic Code. *Annu. Rev.*

Biochem. **2010**, *79* (1), 413–444.

(16)   Murakami, H.; Ohta, A.; Ashigai, H.; Suga, H. A Highly Flexible tRNA Acylation Method

for Non-Natural Polypeptide Synthesis. *Nat. Methods* **2006**, *3* (5), 357–359.

Chapter 2

A Microwell/Printing Fabrication Strategy for the On-Chip Templated Biosynthesis of Protein Microarrays for SPR Imaging

2.1 Introduction

The use of protein microarrays for the study of protein-protein interactions has become a key research tool for many modern biochemical, bioanalytical, and biomedical research laboratories.[1–7] However, for many researchers the preparation of multicomponent protein microarrays via classical protein expression methods is often a significant hurdle. Current methodologies are labor-intensive and require many synthesis and purification steps, in addition to spotting of multiple proteins onto gold thin films. Furthermore, the amount of reagents required in this process is significant, and once fabricated, the protein microarray must be carefully handled to avoid denaturation. In contrast, DNA microarrays are more easily fabricated. Inexpensive DNA, either single-stranded (ssDNA), double stranded (dsDNA) or even modified with various chemical attachment handles or fluorescent tags, are readily available commercially, and DNA microarrays can be stored for long periods of time in the absence of water as compared to their protein-based counterparts.

For this reason, a number of research groups have developed various on-chip multiplexed templated biosynthesis methods that employ DNA microarrays to create protein microarrays using cell-free coupled *in vitro* transcription and translation (IVTT) methods. Some examples include DAPA (DNA array to protein array), [8] NAPPA (nucleic acid programmable protein array), [9,10] and PISA (Protein *In-Situ* Array).[11] In DAPA, protein microarrays are created using IVTT and a dsDNA array to create a protein array *in situ* through a nitrocellulose membrane. NAPPA directly converts a DNA array to a protein array using *in situ* capture of GST-fusion proteins, and PISA utilizes a well-based synthesis method in which proteins are captured *in situ* at the bottom of the well in which they are synthesized. Each of these methods have been

designed to create protein microarrays on glass substrates for analysis by fluorescence or by radioactivity, and have been used in a variety of applications. [4,9,12,13]

While all of these methods are powerful, the applications to date have required the use of either fluorescently or radioactively labeled analytes. In comparison, surface plasmon resonance imaging (SPRI) is a multiplexed surface-sensitive method that detects the adsorption of unmodified biomolecules onto a protein microarray via changes in the local index of refraction, and has been successfully employed in the real-time analysis of either single or multiple bioaffinity adsorption processes.[14-19] The use of unlabeled target analytes in SPRI eliminates any extra label conjugation and purification steps, and also removes any concerns that labeling could perturb the naturally occurring bioaffinity and bioassembly interactions.

The extension of on-chip multiplexed templated biosynthesis methods that create protein microarrays to SPRI measurements would make it significantly easier for researchers to use SPRI in biosensing, biomedical research, and drug discovery applications. With this goal in mind, our group recently published a method of the fabrication of one- and two-component protein microarrays.[20] In this method, microfluidics are used to deliver IVTT solutions to a protein encoding DNA microarray for on-chip biosynthesis. The resulting proteins are captured on-chip by His_6-tags and then used for SPRI analysis.

Since each IVTT-synthesized protein required a unique microfluidic channel, the total number of proteins on a single chip was limited. Thus, there is a need for other methods that can fabricate microarrays with larger numbers of IVTT-synthesized proteins for SPRI measurements.

In this chapter, we demonstrate a method for creating two-dimensional SPRI protein microarrays via an on-chip ribosomal biosynthesis/printing process (shown in Figure 2.1) that is a variation of the DAPA and PISA methods used to create protein microarrays for labeled analysis. We first create a protein *microwell* array by adding IVTT solutions and dsDNA templates to an array of sixteen microwells; each microwell is approximately 0.9 mm in diameter and 0.5 µL in volume. The array is then incubated at 30°C for 30 minutes to produce sixteen
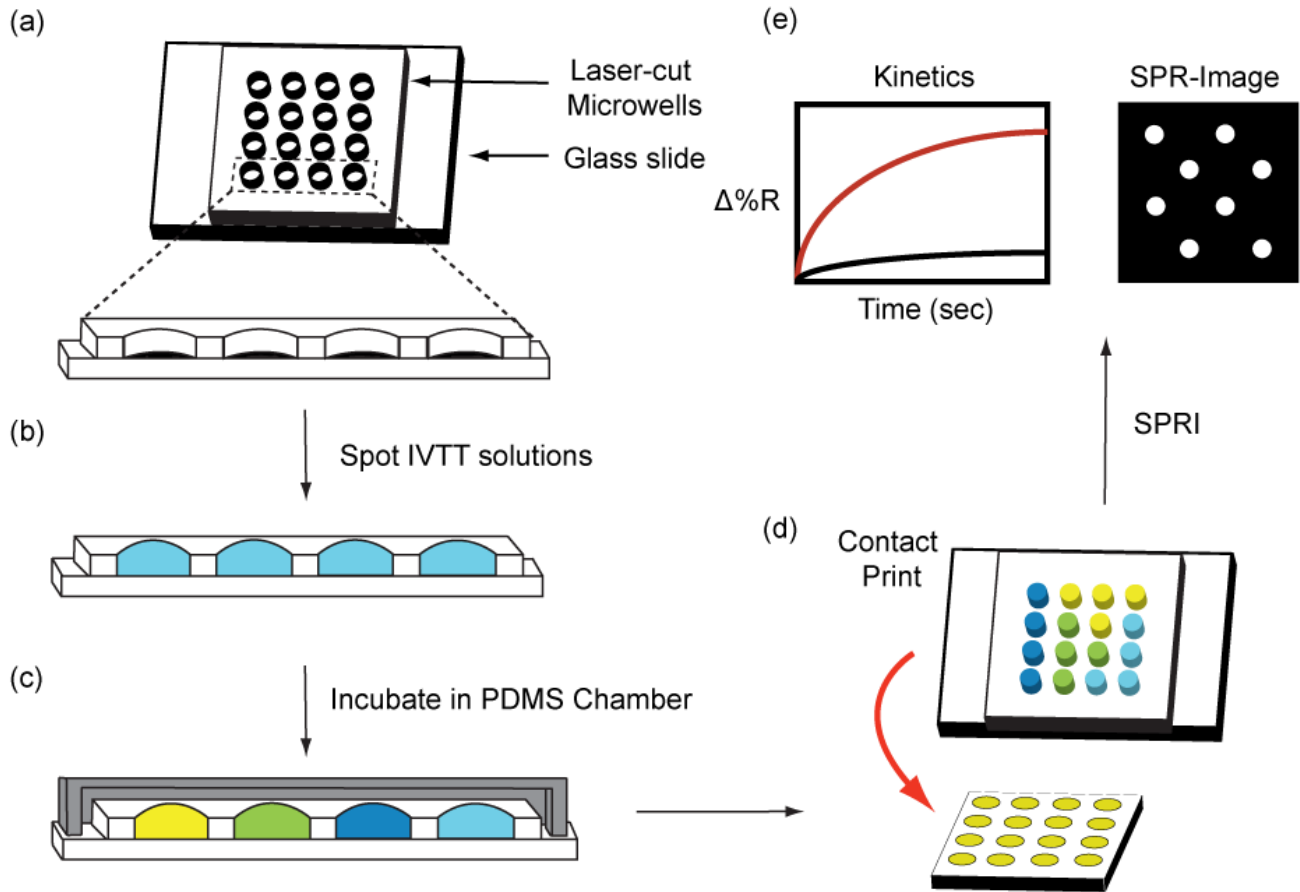
Figure 2.1: On-Chip Biosynthesis and Printing Strategy. (a) Laser-cut polyolefin tape is adhered onto a clean microscope slide to create a 16-element microwell array. (b) In-vitro coupled transcription translation solutions are added to each well. The protein synthesized is dependent upon the DNA included in each well. (c) The microwell is then sealed in a PDMS chamber and incubated at 30°C for 30 minutes. (d) After the incubation period, the chamber is removed and the resulting protein microwell array is contact printed onto an SPR slide. This slide can then be used for SPR measurements (e).

different His-tagged proteins. This resulting protein microwell array is then used to directly print and capture the His-tagged proteins to SPRI chips that consist of NTA-functionalized microarray elements perfectly matched to the spacing and arrangement of the microwell array. As an initial demonstration of this technology, we use multiplexed on-chip templated biosynthesis to create sixteen element "XFP" SPRI protein microarray chips that contain four elements each of wild type green fluorescent protein (GFP), yellow fluorescent protein (YFP), mCherry (RFP), and a control which contain only IVTT reaction solution. These microarray chips are then used in real-time SPRI adsorption measurements to study the binding strength and specificity of various antibodies specific for the structurally related proteins.

2.2 Experimental Considerations

2.2.1 Chemicals and Materials

All chemicals were purchased from Sigma-Aldrich unless otherwise stated. SF-10 glass slides (18 × 18 mm) were purchased from Schott AG. 11-mercaptoundecamine (MUAM) was purchased from Dojindo. N-succinimidyl-S-acetylthiopropionate (SATP) was purchased from Pierce. Maleimide poly-ethyleneglycol (350 Da) was purchased from NanoCS. Maleimido-C3-nitrilotriacetic acid was purchased from Dojindo. Rabbit monoclonal anti-wtGFP was purchased from Santa Cruz Biotechnology. Polyclonal anti-GFP and polyclonal anti-mCherry were purchased from Abcam. pET Biotin His6 mCherry LIC cloning vector (H6-mCherry) was a gift from Scott Gradia (Addgene plasmid #29722). Wild-type GFP, YFP, and TXRED filter cubes were purchased from Thor Labs and used without further modification for the imaging of GFP, YFP and RFP respectively. All water used was obtained by a Milli-Q integral water purification system.

2.2.2 Fabrication of Microwell Arrays

Microwell arrays were laser-cut into 0.2 mm thick polyolefin acrylate Nunc sealing tape (Thermo). The tape was laser cut using a VLS 2.30 laser cutter (Versa Laser) at 4% power. Wells were cut to 0.9 mm diameter with a 1.5 mm center-to-center distance between wells.

2.2.3 YFP Encoding DNA Preparation

DNA encoding YFP was created by mutagenesis of wtGFP DNA. DNA encoding His-tagged wtGFP was obtained from the T7 Rapid Translation System from 5Prime. This vector was then mutagenized to obtain the 10C Q69K YFP variant carrying the following amino acid substitutions: S65G, V68L, Q69K, S72A, and T203Y.[21] The mutations were introduced by PCR site-directed mutagenesis.

2.2.4 Protein Synthesis by *In Vitro* Transcription/Translation

In-vitro coupled transcription/translation (S30 T7 high-yield protein expression system) kits were purchased from Promega. The IVTT reactions were adapted from the manufacturer's recommendation. All components were assembled on ice. 5 μL S30 premix, 4.5 μL of *E. coli.* extract, and 1 μL of glycerol were added to a PCR tube. 0.6 μg of DNA in water was then added followed by dilution to 12.5 μL with water. The reaction was gently mixed, then 0.5 μL of this solution was added to its respective well in the microwell array. This procedure was used for each protein examined in this study.

2.2.5 Fluorescence Measurements

Fluorescence spectra were obtained using a Jasco-6300 Fluorimeter. Fluorescence images were obtained using an Olympus IX-71 fluorescence microscope and an Andor Neo 5.5 sCMOS

detector. A 100 W xenon-arc lamp was used as the light source. Fluorescence filter cubes were purchased from ThorLabs. Images were processed and analyzed by ImageJ.

2.2.6 Preparation of NTA-Functionalized Gold SPRI chips

Nitrilotriacetic acid (NTA) modified SPRI chips were created using a procedure adapted from previous work.[22] SPRI chips were created by treatment of SF10 glass slides with Sigmacote, using the manufacturer's protocol, then by thermally evaporating (Denton DV 502-A evaporator) 1 nm of chromium as an adhesion layer, then 45 nm of gold. These chips were submerged in a 1 mM ethanolic solution of MUAM for 12 h, creating a self-assembled monolayer of terminal amines. The chips were then washed with ethanol and water, and then dried under N_2. A solution of 30 mM NHSS, 150 mM EDC and 14 mM SATP was spotted onto each element. After incubation for 12 h in a humidity chamber, the chip was washed with nanopure water and dried under N_2. A deprotection solution of 25 mM ethylenediaminetriacetic acid (EDTA), 500 mM hydroxylamine, and 50 mM dithiothreitol (DTT) in nanopure water was then added to the SPR chip and incubated in a humidity chamber for 30 min. This solution removes the terminal S-acetyl group to reveal a free thiol surface. After an additional washing and drying step, a solution of 11.25 mM maleimide PEG 350 Da and 3.75 mM maleimido-C3-NTA in PBS and 10% PBS/DMF respectively, was mixed then added to each element and incubated in a humidity chamber for 12 h. This step results in an NTA/PEG functionalized surface. Before protein capture, each element is exposed to a 40 mM $CuSO_4$ aqueous solution for 15 minutes, which is required for His_6-tag affinity purification.

2.2.7 On-Chip Synthesis and Protein Microarray Printing.

In-vitro coupled transcription/translation (S30 T7 high-yield protein expression system) kits were purchased from Promega. The IVTT reactions were adapted from the manufacturer's recommendation. All components were assembled on ice. 5 µL S30 premix, 4.5 µL of *E. coli.* extract, and 1 µL of glycerol were added to a PCR tube. 0.6 µg of DNA in water was then added followed by dilution to 12.5 µL with water. The reaction was gently mixed, then 0.5 µL was added to its respective well in the microwell array. The microwell array was sealed in a PDMS chamber and incubated at 30°C for 30 minutes. The PDMS chamber was removed and the array was placed in a humidity chamber. The array and chamber were incubated at 4°C for at least 2 hours to allow for protein folding.

A 0.25-mm thick, square spacer (1.0 x 1.0 cm) (ThermoFisher) is adhered to the protein microwell array. The array is then inverted and contacted printed onto an NTA-functionalized SPRI chip. The array is allowed to print at 25°C for 15 minutes in a humidity chamber. The microwell array is removed and stored at 4°C to be reused.

The amount of protein produced by this method was determined by fluorescence intensity. After on-chip biosynthesis, the solutions were removed and diluted into 60 µL of PBS. These solutions were then analyzed for fluorescence and compared to the fluorescence of a known concentration of XFP.

2.2.8 SPRI Apparatus

The real-time SPRI measurements were obtained with an SPRimager instrument from GWC Technologies (Madison, WI) as described previously.[23]

2.2.9 Solutions and Chemicals for the SPRI anti-XFP Antibody Binding Measurements

Before antibody analysis by SPRI, the protein microarray is added to the SPRimager instrument. The protein microarray is then washed with various solutions using the instrument's microfluidic pumps. The array is first washed with aqueous solution of 50 mM sodium phosphate, 300 mM NaCl, pH 6.0, then with 0.5% solution of Tween-20 in PBS, followed by PBS. Antibodies were diluted to 1 nM in PBS and used without further modification.

2.3 Results and Discussion

2.3.1 Strategy for Fabricating Protein Microwell Arrays for SPRI

Our overall strategy for obtaining SPRI bioaffinity adsorption measurements with protein microarrays created by on-chip templated biosynthesis and contact printing is outlined in Figure 2.1. The first step is to create a protein microwell array using on-chip IVTT. This preparation methodology is similar to previously reported methods for the fabrication of protein microarrays for fluorescence microscopy, DAPA[8], NAPPA[10] and PISA[11]. The sixteen-element microwell array was created by laser-cutting sixteen 0.9 mm diameter holes in a 4×4 grid into poly-olefin sealing tape that was subsequently attached to a clean microscope slide (Figure 2.1a). These chips were then used for simultaneous on-chip synthesis of multiple proteins using commercially available IVTT solutions. Each microwell was spotted with 0.5 µL of a solution that contained both the IVTT mix and approximately 350 femtomoles of a dsDNA template (Figure 2.1b). These dsDNA templates encode a specific protein modified with a N-terminal His_6-tag that will be used for surface affinity capture onto the SPRI chip. The microwell array was then sealed in a poly(dimethylsiloxane) (PDMS) chamber to prevent evaporation, and protein synthesis was performed by incubating the sealed microwell array at 30°C for 30 minutes followed by

incubation at 4°C for 12 hours to allow for protein folding (Figure 2.1c). The PDMS chamber was then removed and the resultant protein microwell array was either checked directly with fluorescence microscopy or employed in the printing of SPRI chips (Figure 2.1d).

2.3.2 Demonstration Part 1: Fabrication of XFP Protein Microwell Microarrays

In order to track the effectiveness of this method, an "XFP" protein microwell array of three related and well-studied fluorescence proteins were chosen: GFP, YFP and RFP. Choosing three proteins each with a unique fluorescence spectrum[21,24] allowed us to easily confirm successful on-chip IVTT protein synthesis and the correct folding of the IVTT-synthesized proteins. The fluorescence spectra of these three IVTT-synthesized proteins are shown in Figure
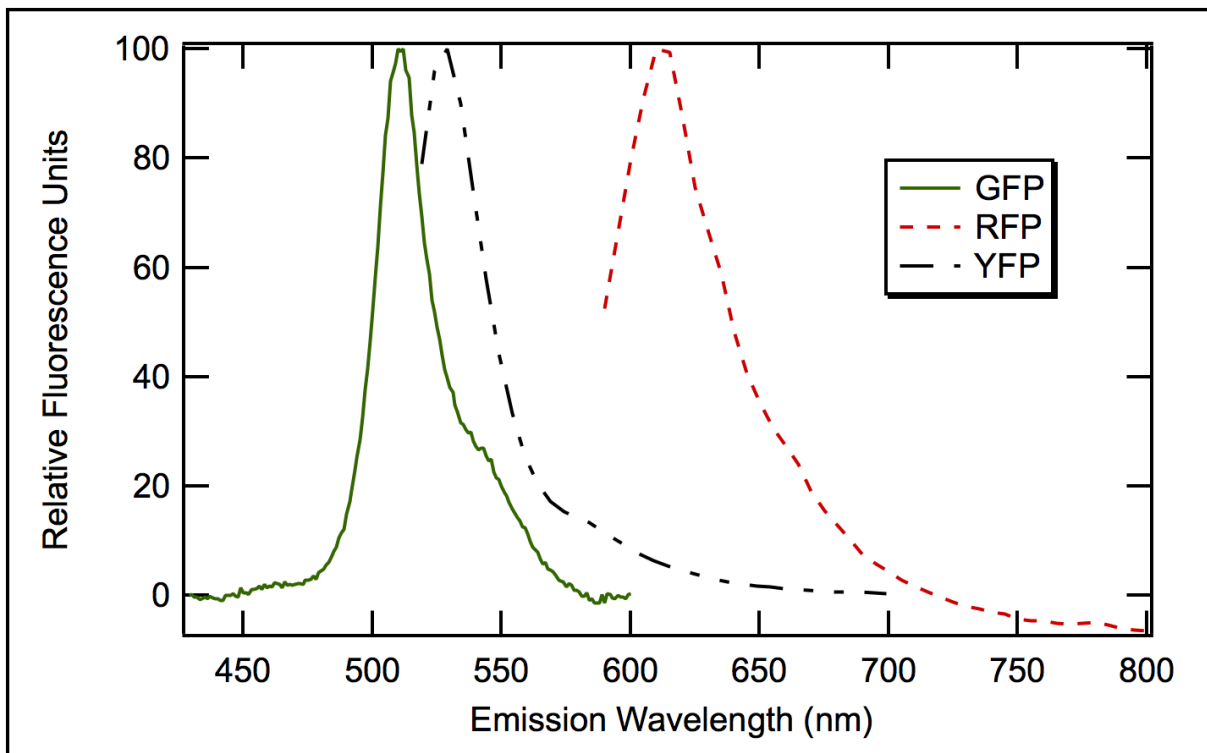
Figure 2.2: Fluorescence Spectra of GFP, YFP, and RFP: Normalized fluorescence emission spectra of GFP, YFP, and RFP. Emission was measured at 395 ± 10 nm, 516 ± 10 nm, and 570 ± 10 nm respectively. The proteins were synthesized using a cell free coupled transcription/translation system, then diluted into 60 µL of PBS. These solutions were then measured for fluorescence by fluorometer.
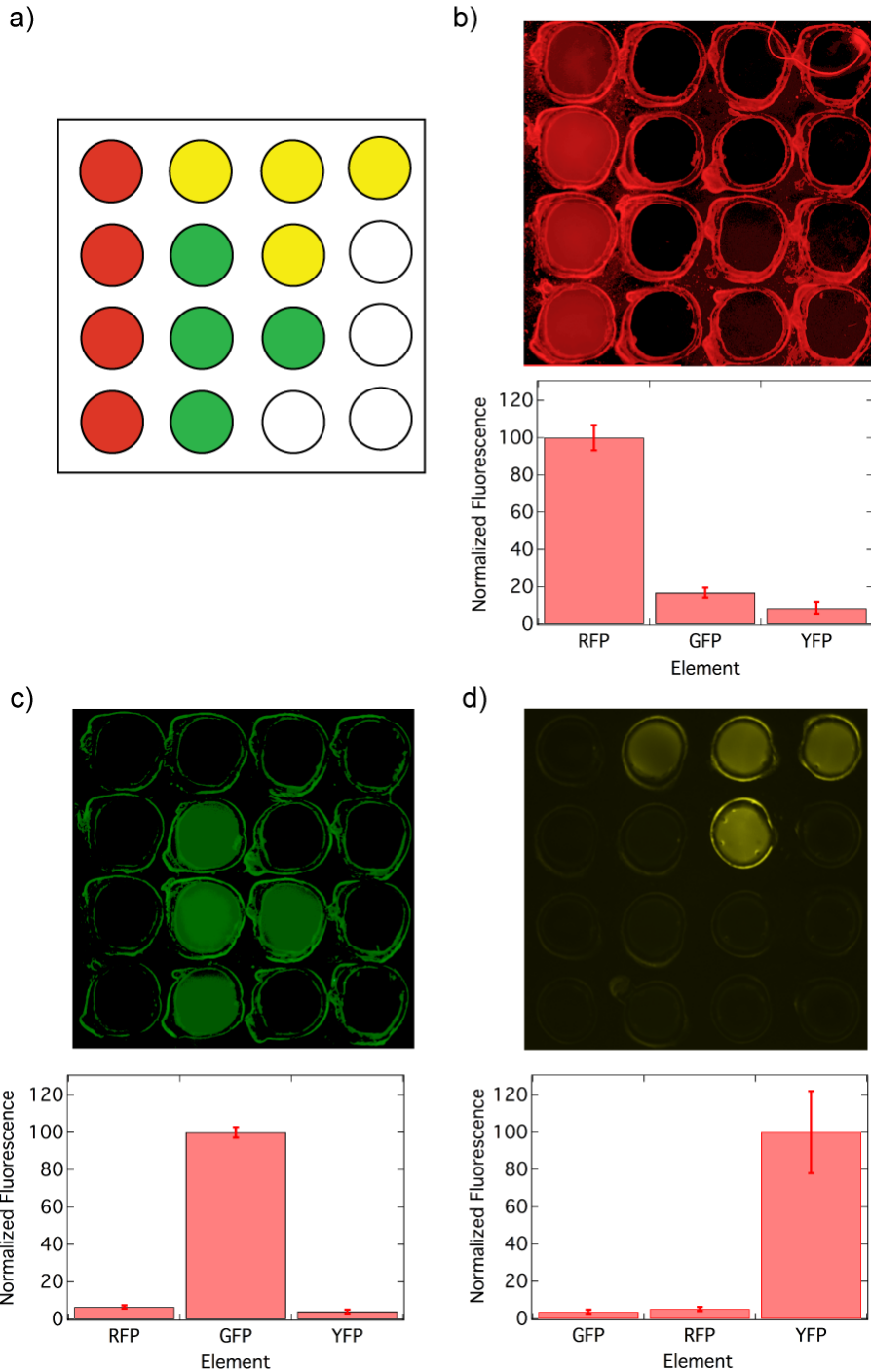
Figure 2.3: Fluorescence Images of the XFP protein microwell array. Fluorescence images of (a) RFP, (b) GFP, and (c) YFP were obtained after on-chip synthesis and incubation for 12 hrs at 4°C. Images were obtained via fluorescence microscopy using the appropriate fluorescence filter cubes for each protein with a 2x objective. Quantitative data was obtained by measuring average fluorescence intensity for each protein under each fluorescence filter (Filters used are outlined in experimental section). Melting during the laser cutting process caused the shape distortion observed in the microwell arrays. This distortion did not affect IVTT or the contact printing process.

2.2. The multiplexed on-chip IVTT method described above was used to synthesize a 16-element, four component "XFP" microwell array containing GFP, YFP, and RFP, along with non-fluorescent control wells. A series of fluorescence images of an XFP microwell array utilizing different excitation and emission filters is shown in Figure 2.3; the quantitative analysis (bar graphs) of these images are shown in Figure 2.3 as well and verify the efficient multiplexed biosynthesis of these fluorescent proteins. The solutions were removed from the wells and by comparing with fluorescence from IVTT standards (see Experimental Section for details) we estimate that approximately 40 ± 10 picomoles of protein was synthesized in each microwell from 350 femtomoles of DNA templates; the variation in this number is attributed to differences in the efficiency of synthesizing the various proteins from dsDNA templates. Forty picomoles in 0.5 microliters corresponds to an 80 micromolar protein solution in each well that was used for the printing of SPRI chip microarrays.

2.3.3 Strategy for Fabricating SPRI Protein Chips from Protein Microwell Arrays

As shown in Figure 2.1, we created protein microarrays on SPRI chips by contact printing from the protein microwell arrays; the SPRI chips had 16 gold thin film elements that matched the pattern of the microwell arrays. His-tagged proteins are captured onto the SPRI chip by Cu[II]-NTA-functionalized microarray elements. Maleimide-functionalized NTA was attached to the gold thin film microarray elements using a SATP strategy (Figure 2.4) that has been described and characterized previously.[22] The SPRI chips also include a thin hydrophobic Sigmacote film on the glass areas surrounding the gold microarray elements to prevent crosstalk during the fabrication process.[19] The NTA-functionalized chips were exposed to an aqueous 40
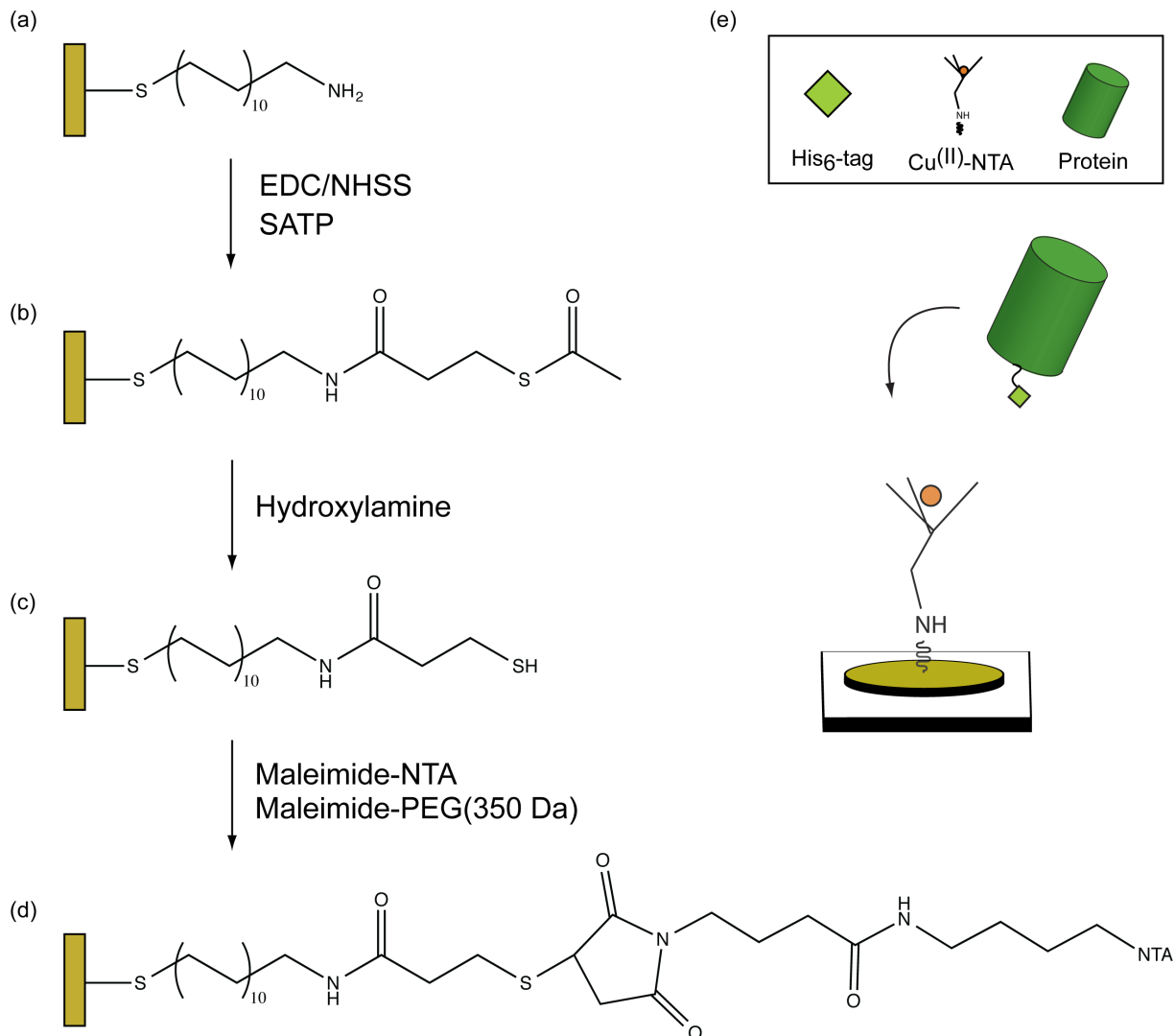
Figure 2.4: Surface attachment chemistry for printing SPRI protein microarrays from the protein microwell array. Surface attachment chemistry was adapted from previous methods[22]. (a) A self-assembled monolayer of 11-mercaptoundecamine was formed on a gold thin-film SPRI element. (b) The resulting amine surface was modified with SATP, a heterobifunctional linker, using EDC/NHSS chemistry. (c) The surface terminal S-acetyl group is removed using a hydroxylamine solution, revealing a free thiol. (d) The revealed thiol surface is treated with a solution of maleimido-nitrilotriacetic acid and maleimido-polyethylene glycol (350). (e) This surface is then exposed to a 4 mM solution of Cu^{II}, which primes the surface for His-tag capture.

mM Cu^{II} solution for 15 minutes and then rinsed with nanopure water. Then, a 0.25-mm thick, square spacer (1.0 x 1.0 cm) (ThermoFisher) was placed around the microwell array to prevent crosstalk between wells by reducing droplet compression. The microwell array was then placed, wells facing down, on top of a 16-element, NTA-functionalized SPRI chip. This insured that each well spotted a single solution onto a single SPRI element. The coupled printing/capture arrays were incubated in a humidity chamber at 25°C for 15 minutes to allow for NTA-capture of the proteins onto the SPRI chip. The chip was subsequently washed with various solutions outlined in the Experimental Section and then used in SPRI experiments. Multiple (up to 3) SPRI chips could be fabricated from a single protein microwell array.

In the process of optimizing the conditions for this parallel on-chip IVTT microwell biosynthesis and subsequent SPRI chip printing, several hurdles needed to be overcome to create a successful and repeatable fabrication process: (1) the reduction of evaporation losses, (2) mass transfer ("coffee-ring") effects, (3) crosstalk between microarray elements, and (4) inefficient His-tag protein adsorption/desorption kinetics onto the SPRI elements. Losses from evaporation were prevented by both the use of a humidity chamber and the addition of glycerol (~10% of the total solution) to the protein microwell solutions before the incubation step. The use of glycerol to minimize evaporation issues has been employed previously in various drop-based microarray synthesis methods.[25–27] The addition of glycerol coupled with a short reaction time (30 minutes) also alleviated the localization of protein molecules into a ring at the edges of the wells (Figure 2.5). This localization has been observed previously and explained as a "coffee-ring" effect by other researchers.[28,29] To prevent crosstalk caused by bleeding of adjacent protein microwells

a) - glycerol
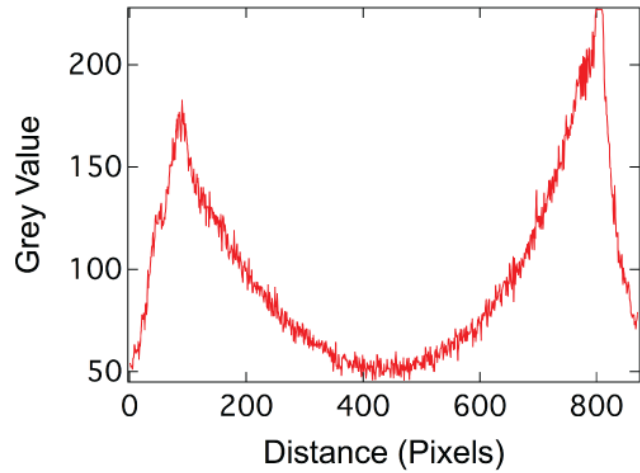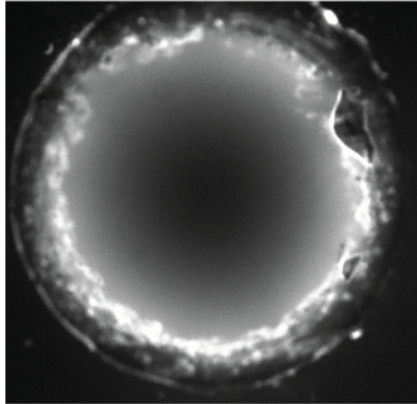
b) + glycerol
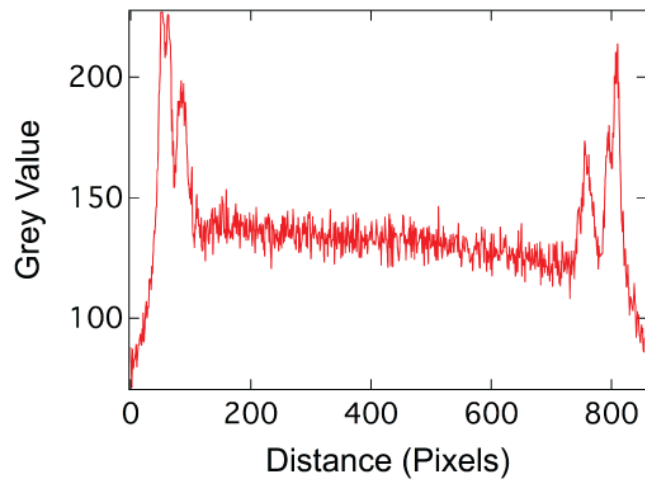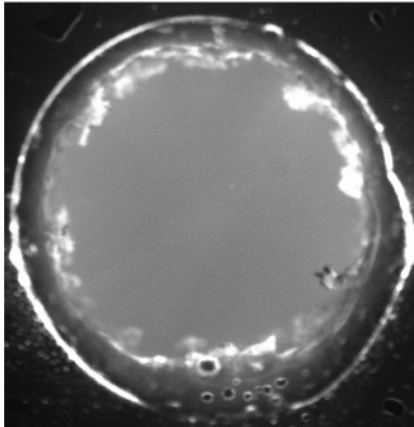
Figure 2.5: Demonstration of Coffee Ring Effect and Prevention by Glycerol Addition. On-chip biosynthesis of GFP was performed in a 16-element microwell array. Experiment was performed as written in the Experimental Section. (a) Fluorescence image and cross-sectional intensity of GFP emission. Upon observation under a fluorescence microscope, we observe coffee ring effects. A line profile quantitates our observations, showing a gradual decrease in GFP fluorescence moving away from the center of the microwell. (b) Fluorescence image and cross-sectional intensity of GFP emission with glycerol added to the IVTT solution prior to incubation. We see a uniform distribution of fluorescence throughout the well, indicating prevention of coffee ring effects by glycerol addition

into other elements by droplet compression, a 0.25 mm thick spacer was placed between the microwell array and the surface of the SPRI chip. Additionally, a 1.5 mm center-to-center distance between the 0.9 mm diameter microarray elements was used; this spacing/diameter ratio yielded the maximum microarray element density while still completely preventing crosstalk. And finally, since the His-tag capture of the proteins onto the SPRI microarray elements is itself a bioaffinity adsorption process, losses due to slow Langmuir adsorption kinetics were avoided by using a high (80 micromolar) protein solution. Moreover, to avoid the reversible desorption of His-tagged proteins that has been observed previously from Ni-NTA modified surfaces,[30] we substituted Ni^{2+} with Cu^{2+} which has been shown to form less labile affinity capture complexes with His-tagged proteins.[31]

2.3.4 Demonstration Part 2: SPRI Measurements of Antibody Binding to the XFP Chips.

In order to demonstrate the utility of these contact printed, multiplexed protein SPRI microarrays, we examined the adsorption of antibodies onto various XFP SPRI chips with real-time SPRI measurements. We first examined the efficiency of our contact printing method with a sixteen element, two component protein microarray that contained 8 elements of IVTT synthesized GFP and 8 control elements of IVTT solutions alone. The SPRI real-time reflectivity change (Δ%R) was measured over the course of 900 s upon exposure of the microarray to a one nanomolar solution of monoclonal anti-GFP; Figure 2.6 shows the two average Δ%R curves for the eight GFP and eight control elements. An increase in Δ%R of up to 1.6% after 600 s was observed for the GFP elements, and a small increase (~0.1 increase in Δ%R) was observed from the control elements. These results match well with our previous SPRI on-chip biosynthesis using channels.[20] A final Δ%R value of 1.6% from a 1 nM anti-GFP solution compares favorably
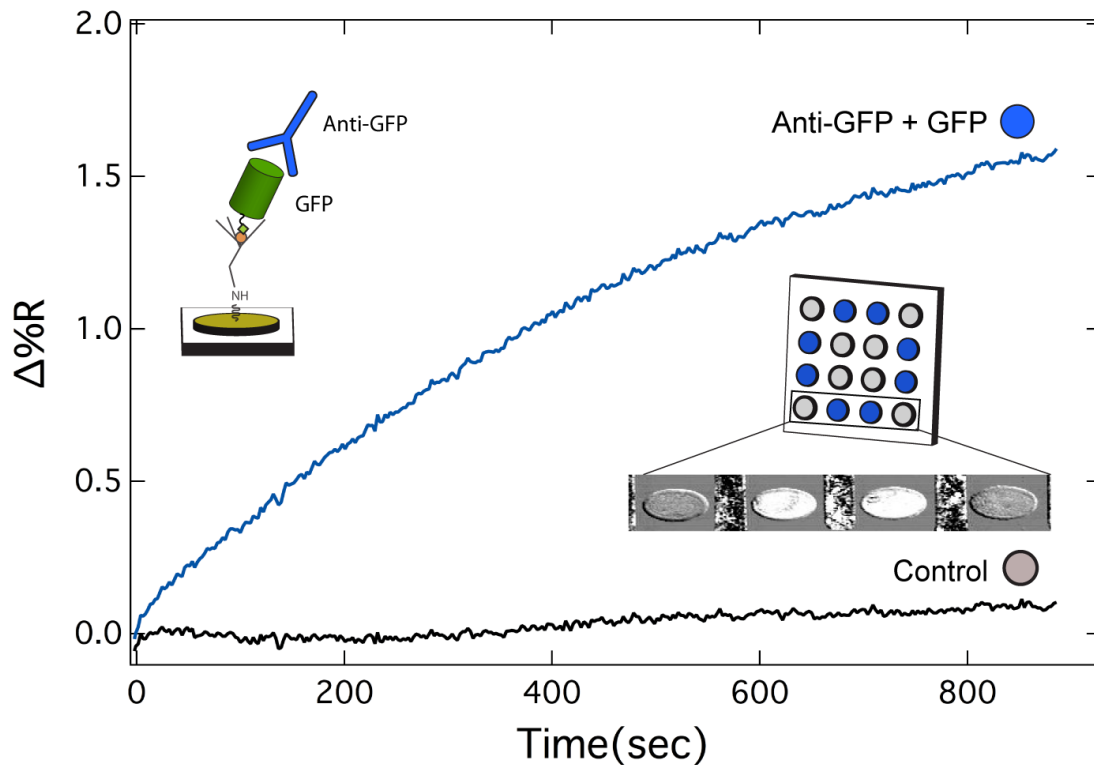
Figure 2.6 Real-Time SPRI measurements monoclonal anti-GFP onto a GFP microarray SPRI chip. As a proof of concept for our printing method, we contact-printed a microwell array of GFP to a functionalized SPRI chip. This SPRI chip was then exposed to 1 nM monoclonal anti- GFP. We observe a $\Delta\%R$ of 1.6% for elements printed with GFP, while elements printed with only IVTT mix produced a $\Delta\%R$ of 0.1%

with previous SPRI measurements of adsorbed probe protein surface densities of approximately 10^{12} molecules cm^{-2}.[23, 32] Using this number as an upper limit, we estimate that there is approximately 100 femtomoles of GFP adsorbed onto each gold SPRI chip element. The SPRI difference image shown as an inset in Figure 2.6 also verifies by SPRI measurements of the specific adsorption of anti-GFP to the printed GFP elements, that there is no crosstalk between the elements due to the printing process. In a second set of real-time SPRI measurements we monitored the adsorption of various antibodies onto XFP chips created from the protein microwell arrays in Section 2.3.3. Sixteen-element SPRI microarray chips which contained four elements each of GFP, YFP, RFP and a no-protein control were contact-printed. These XFP

chips were then used in real-time SPRI reflectivity measurements to examine the specific adsorption of three antibodies: monoclonal anti-GFP, polyclonal anti-GFP, and polyclonal anti-mCherry. The results of these antibody binding measurements are plotted in Figure 2.7a, 2.7b, and 2.7c respectively. One nanomolar antibody solutions in PBS were used in each of these experiments. As seen in Figure 2.7a, monoclonal anti-GFP preferentially adsorbed to the GFP elements (after 1100 s, Δ%R values of 0.8 ± 0.2%, 0.20 ± 0.08%, and 0.03 ± 0.08% , for GFP, YFP, and RFP respectively). The 4X preference for this antibody to GFP elements over YFP elements is significant given the similarity between the two proteins; GFP and YFP differ by only six residues and many of these amino acids are buried within the beta-barrel structure.[33,34] In contrast, the real-time SPRI measurements plotted in Figure 2.7b of polyclonal anti-GFP binding onto XFP chips shows similar adsorption to both GFP and YFP elements (after 1100 s, Δ%R values of 0.3 ± 0.1%, 0.3 ± 0.1%, and 0.00 ± 0.09%, for GFP, YFP, and RFP respectively). Finally, the real-time SPRI measurements in Figure 2.7c demonstrate that the exposure of the XFP chip to 1 nM polyclonal anti-RFP, leads only to specific adsorption to RFP elements (after 1100 s, Δ%R values of 0.06 ± 0.03%, 0.01 ± 0.07%, and 0.6 ± 0.2%, for GFP, YFP, and RFP respectively). This specificity is attributed to RFP's unique primary structure as compared to GFP and YFP, even though the three share a similar beta-barrel structure.[24,34]

We attribute the 4× preference of monoclonal anti-GFP to GFP over YFP to a change in

the tertiary structure of YFP upon introduction of the six amino acid substitutions described in

the experimental section. Upon examination of the crystal structure of wtGFP, we find the

peptide backbone of position 203 is solvent exposed. We suspect that upon the T203Y change, a

change in the tertiary structure of YFP must cause the observed monoclonal GFP specificity.

This selectivity was not observed with polyclonal anti-GFP serum because it is a heterogeneous

mixture of antibodies that interact with a variety of epitopes; some of these interactions are
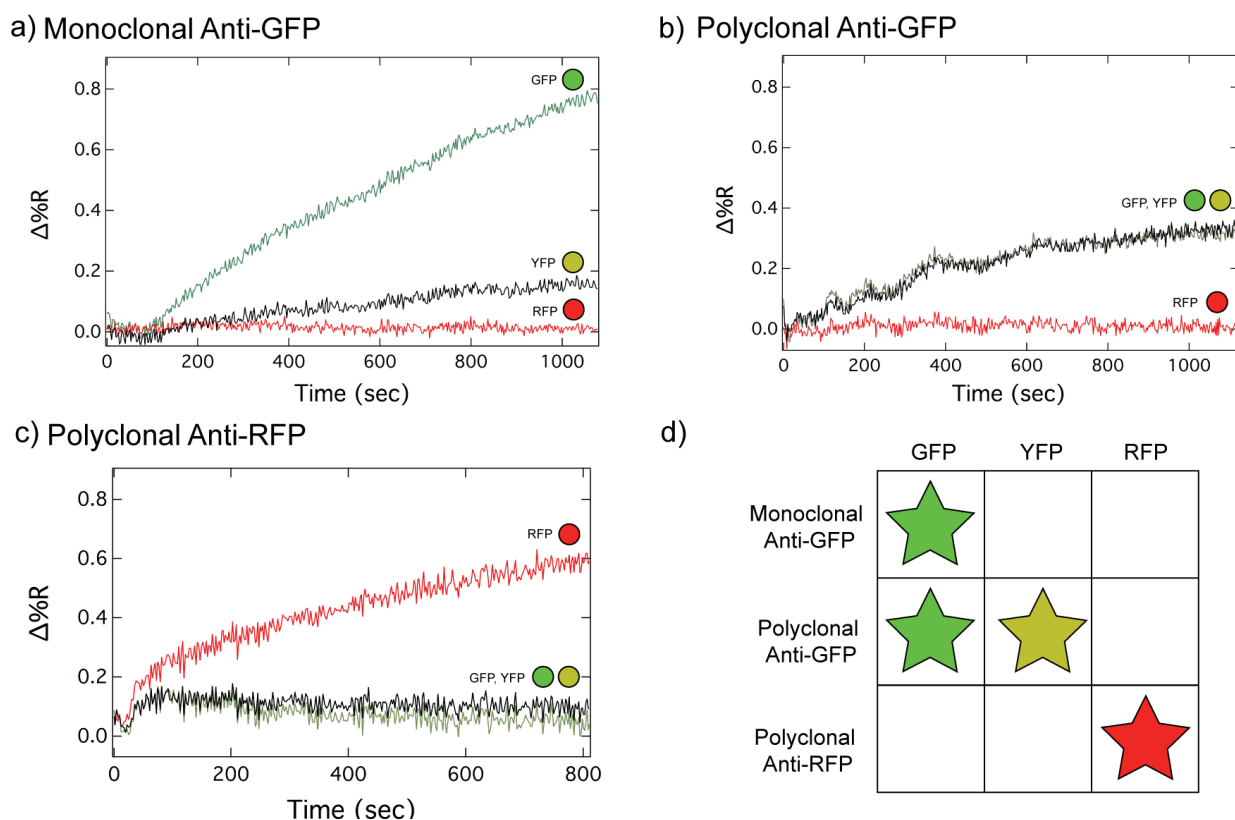
Figure 2.7: Real-time SPRI measurements of the adsorption of various antibodies onto a XFP microarray SPRI chip. After on-chip synthesis of a multi-protein microwell array, the array was printed onto a functionalized SPRI chip and real-time SPRI measurements were performed. (a) Real-time SPRI measurements of the adsorption of 1nM monoclonal anti-GFP to a printed protein microarray. (b) Real-time SPRI measurements of the adsorption of 1 nM polyclonal anti-GFP. (c) Real-time SPRI measurements of the adsorption of 1 nM polyclonal anti-GFP. (d) We observe specificity of monoclonal anti-GFP only to GFP elements, while polyclonal-GFP is specifically adsorbs to both GFP and YFP. Polyclonal-RFP is specific for RFP. The specificity observed in these experiments was reproducible in 3 replicates.

insensitive to the structural differences between YFP and GFP.

This set of SPRI measurements of antibody adsorption on the XFP chips clearly demonstrates that the SPRI protein microarrays created via the biosynthesis/printing methodology described in this chapter can be used in multiplexed protein-protein SPRI bioaffinity measurements.

2.4 Conclusions

In this chapter, we describe a two-step methodology for fabricating protein microarrays for SPRI measurements via multiplexed templated IVTT biosynthesis of His-tagged proteins in a microwell array followed by contact printing/adsorption onto an NTA-modified gold thin film SPRI chip. This method is a simple and attractive method for any researcher interested in quickly producing a variety of different protein microarrays for SPRI measurements with a minimum of reagents, processing and purification steps. The surface density of the proteins for SPRI protein microarrays needs to be higher than for the DAPA or PISA protein microarrays used in previously for fluorescence imaging experiments; the high concentration (80 micromolar) of the synthesized proteins in each microwell insures a significant surface coverage of captured and active his-tagged proteins. This high concentration also permits the fabrication of multiple SPRI chips as each SPRI microarray element only requires approximately 100 femtomoles of adsorbed protein.

As compared to our previous microfluidic method for the fabrication of SPRI microarrays with IVTT templated biosynthesis, this contact printing method is easier to implement for larger microarrays (16 or more) of proteins. However, both methods suffer from the fact that we only use one type of protein adsorption chemistry, namely the adsorption of His-tagged proteins onto

a Cu^{II} NTA-modified gold surface. The ultimate goal of creating **self-assembled** SPRI microarrays in a single on-chip templated IVTT biosynthesis will require the future development of simultaneous multiple adsorption chemistries, perhaps through the addition of a ssDNA capture tag to each type of synthesized protein.

2.5 Acknowledgements

2.6 References

(1) Hall, D. A.; Ptacek, J.; Snyder, M. Protein Microarray Technology. *Mech. Ageing Dev.* **2007**, *128* (1), 161–167.

(2) Kingsmore, S. F. Multiplexed Protein Measurement: Technologies and Applications of Protein and Antibody Arrays. *Nat. Rev. Drug Discov.* **2006**, *5* (4), 310–321.

(3) Angenendt, P. Progress in Protein and Antibody Microarray Technology. *Drug Discov. Today* **2005**, *10* (7), 503–511.

(4) Wilson, D. S.; Nock, S. Recent Developments in Protein Microarray Technology. *Angew. Chem. Int. Ed.* **2003**, *42* (5), 494–500.

(5) Phizicky, E.; Bastiaens, P. I. H.; Zhu, H.; Snyder, M.; Fields, S. Protein Analysis on a Proteomic Scale. *Nature* **2003**, *422* (6928), 208–215.

(6) Kodadek, T. Protein Microarrays: Prospects and Problems. *Chem. Biol.* **2001**, *8* (2), 105–115.

(7) Emili, A. Q.; Cagney, G. Large-Scale Functional Analysis Using Peptide or Protein Arrays. *Nat. Biotechnol.* **2000**, *18* (4), 393–397.

(8) Schmidt, R.; Cook, E. A.; Kastelic, D.; Taussig, M. J.; Stoevesandt, O. Optimised "on Demand" Protein Arraying from DNA by Cell Free Expression with the "DNA to Protein Array" (DAPA) Technology. *J. Proteomics* **2013**, *88*, 141–148.

(9) Olia, A. S.; Barker, K.; McCullough, C. E.; Tang, H.-Y.; Speicher, D. W.; Qiu, J.; LaBaer, J.; Marmorstein, R. Nonenzymatic Protein Acetylation Detected by NAPPA Protein Arrays. *ACS Chem. Biol.* **2015**, *10* (9), 2034–2047.

(10) Yu, X.; LaBaer, J. High-Throughput Identification of Proteins with AMPylation Using Self-Assembled Human Protein (NAPPA) Microarrays. *Nat. Protoc.* **2015**, *10* (5), 756–767.

(11) He, M.; Taussig, M. J. Single Step Generation of Protein Arrays from DNA by Cell-Free Expression and in Situ Immobilisation (PISA Method). *Nucleic Acids Res.* **2001**, *29* (15), e73.

(12) Ramachandran, N.; Hainsworth, E.; Bhullar, B.; Eisenstein, S.; Rosen, B.; Lau, A. Y.; Walter, J. C.; LaBaer, J. Self-Assembling Protein Microarrays. *Science* **2004**, *305* (5680), 86–90.

(13) Ramachandran, N.; Raphael, J. V.; Hainsworth, E.; Demirkan, G.; Fuentes, M. G.; Rolfs, A.; Hu, Y.; LaBaer, J. Next-Generation High-Density Self-Assembling Functional Protein Arrays. *Nat. Methods* **2008**, *5* (6), 535–538.

(14) Singh, P. SPR Biosensors: Historical Perspectives and Current Challenges. *Sens. Actuators B Chem.* **2016**, *229*, 110–130.

(15) Fasoli, J. B.; Corn, R. M. Surface Enzyme Chemistries for Ultrasensitive Microarray Biosensing with SPR Imaging. *Langmuir* **2015**, *31* (35), 9527–9536.

(16) Halpern, A. R.; Wood, J. B.; Wang, Y.; Corn, R. M. Single-Nanoparticle Near-Infrared Surface Plasmon Resonance Microscopy for Real-Time Measurements of DNA Hybridization Adsorption. *ACS Nano* **2014**, *8* (1), 1022–1030.

(17) Chen, Y.; Nakamoto, K.; Niwa, O.; Corn, R. M. On-Chip Synthesis of RNA Aptamer Microarrays for Multiplexed Protein Biosensing with SPR Imaging Measurements. *Langmuir* **2012**, *28* (22), 8281–8285.

(18) Seefeld, T. H.; Zhou, W.-J.; Corn, R. M. Rapid Microarray Detection of DNA and Proteins in Microliter Volumes with Surface Plasmon Resonance Imaging Measurements. *Langmuir* **2011**, *27* (10), 6534–6540.

(19) Chen, Y.; Nguyen, A.; Niu, L.; Corn, R. M. Fabrication of DNA Microarrays with Poly(l-Glutamic Acid) Monolayers on Gold Substrates for SPR Imaging Measurements. *Langmuir* **2009**, *25* (9), 5054–5060.

(20) Seefeld, T. H.; Halpern, A. R.; Corn, R. M. On-Chip Synthesis of Protein Microarrays from DNA Microarrays via Coupled In Vitro Transcription and Translation for Surface Plasmon Resonance Imaging Biosensor Applications. *J. Am. Chem. Soc.* **2012**, *134* (30), 12358–12361.

(21) Tsien, R. Y. The Green Fluorescent Protein. *Annu. Rev. Biochem.* **1998**, *67* (1), 509–544.

(22) Wegner, G. J.; Lee, H. J.; Marriott, G.; Corn, R. M. Fabrication of Histidine-Tagged Fusion Protein Arrays for Surface Plasmon Resonance Imaging Studies of Protein−Protein and Protein−DNA Interactions. *Anal. Chem.* **2003**, *75* (18), 4740–4746.

(23) Lee, H. J.; Nedelkov, D.; Corn, R. M. Surface Plasmon Resonance Imaging Measurements of Antibody Arrays for the Multiplexed Detection of Low Molecular Weight Protein Biomarkers. *Anal. Chem.* **2006**, *78* (18), 6504–6510.

(24) Shu, X.; Shaner, N. C.; Yarbrough, C. A.; Tsien, R. Y.; Remington, S. J. Novel Chromophores and Buried Charges Control Color in mFruits,. *Biochemistry (Mosc.)* **2006**, *45* (32), 9639–9647.

(25) Wu, P.; Grainger, D. W. Comparison of Hydroxylated Print Additives on Antibody Microarray Performance. *J. Proteome Res.* **2006**, *5* (11), 2956–2965.

(26) Lee, C.-S.; Kim, B.-G. Improvement of Protein Stability in Protein Microarrays. *Biotechnol. Lett.* **2002**, *24* (10), 839–844.

(27) MacBeath, G.; Schreiber, S. L. Printing Proteins as Microarrays for High-Throughput Function Determination. *Science* **2000**, *289* (5485), 1760–1763.

(28) Yunker, P. J.; Still, T.; Lohr, M. A.; Yodh, A. G. Suppression of the Coffee-Ring Effect by Shape-Dependent Capillary Interactions. *Nature* **2011**, *476* (7360), 308–311.

(29) Deegan, R. D.; Bakajin, O.; Dupont, T. F.; Huber, G.; Nagel, S. R.; Witten, T. A. Capillary Flow as the Cause of Ring Stains from Dried Liquid Drops. *Nature* **1997**, *389* (6653), 827–829.

(30) Khan, F.; He, M.; Taussig, M. J. Double-Hexahistidine Tag with High-Affinity Binding for Protein Immobilization, Purification, and Detection on Ni−Nitrilotriacetic Acid Surfaces. *Anal. Chem.* **2006**, *78* (9), 3072–3079.

(31) Ueda, E. K. .; Gout, P. .; Morganti, L. Current and Prospective Applications of Metal Ion–protein Binding. *J. Chromatogr. A* **2003**, *988* (1), 1–23.

(32) Li, Y.; Lee, H. J.; Corn, R. M. Fabrication and Characterization of RNA Aptamer Microarrays for the Study of Protein–aptamer Interactions with SPR Imaging. *Nucleic Acids Res.* **2006**, *34* (22), 6416–6424.

(33) Heim, R.; Tsien, R. Y. Engineering Green Fluorescent Protein for Improved Brightness, Longer Wavelengths and Fluorescence Resonance Energy Transfer. *Curr. Biol.* **1996**, *6* (2), 178–182.

(34) Ormö, M.; Cubitt, A. B.; Kallio, K.; Gross, L. A.; Tsien, R. Y.; Remington, S. J. Crystal Structure of the Aequorea Victoria Green Fluorescent Protein. *Science* **1996**, *273* (5280), 1392–1395.

Chapter 3

Self-Assembly of Protein Microarrays Directed by Zinc Finger-DNA Bioaffinity

3.1 Introduction

Multiplexed surface bioaffinity measurements that employ either DNA or protein microarrays are powerful methods for the simultaneous detection and analysis of multiple proteins or DNAs in a single experiment.[1–5] These microarrays can be quite large, sometimes encompassing entire genomes, but smaller microarrays (tens or hundreds of proteins or DNAs) are often required for more specific biosensing and bioaffinity interaction studies. While there are now fairly straightforward methods for the synthesis and fabrication of these smaller DNA microarrays,[6,7] the fabrication of protein microarrays is still an arduous process that requires extensive protein biosynthesis, purification, and spotting.

Recently, new methods that employ coupled *in vitro* transcription and translation (IVTT) have been developed for the creation of protein microarrays for fluorescence and surface plasmon resonance imaging (SPRI) biosensing,[8] but these methods still require synthesis of proteins in separate wells,[9] spots,[10–12] or microfluidic channels[13] to achieve the spatial selectivity required for microarrays. Various solutions have been developed for this spatial selectivity problem, with the vast majority of research groups opting for on-chip protein biosynthesis and "just-in-time" capture using various universal affinity tags (identical capture tags on each protein in an array), such as the His_6-tag or the GST-fusion tag.[13–19] However, the use of universal affinity tags for protein capture carries inherent issues, such as diffusion based cross-contamination between two or more array elements and complicated array fabrication processes, which have hindered widespread adoption.

A transition to using unique, orthogonal capture tags for each protein in an array would address these issues and have additional advantages. First, the self-assembly of the protein microarray would reduce the need for either manual or robotic spotting of proteins on the

37

microarray chip, reducing the fabrication complexity. Second, the synthesis of the entire set of proteins needed for the microarray could occur simultaneously in a single IVTT experiment in approximately 50 µL using common laboratory equipment, greatly simplifying protein preparation. Third, unique orthogonal capture tags have potential uses outside protein microarrays, such as in the decoration of nanostructured surfaces with high spatial selectivity. This application is particularly interesting in the context of pathogen recognition processes by the innate immune system, which has recently been found to be sensitive to the spatial organization of pathogen-associated molecules.[20] These reasons provide the motivation to develop a new capture chemistry for proteins.

In this chapter, we introduce a new protein capture chemistry, based on zinc finger/DNA bioaffinity, and demonstrate how the sequence-specific binding of zinc finger fusion proteins (ZFPs) to double-stranded DNA (dsDNA) microarrays can be used for the self-assembly of protein microarrays.

Zinc fingers (ZFs) are widespread protein motifs found throughout nature that are capable of binding dsDNA with high sequence specificity, deriving their name from their dependence on Zn^{II} for proper folding.[21] There are many structural classes of zinc fingers, the most common being the Cys_2His_2 class. In this class of ZF, 2 cysteines and 2 histidines coordinate to a Zn^{II} center, which is essential for adopting a functional ββα-type fold for DNA recognition. Residues within the α-helix of this fold make sequence specific contacts with bases in the major groove of dsDNA.[22–27] Researchers have recognized the potential of artificial ZFs with tunable DNA binding capabilities and have realized this potential by changing the residues in the DNA recognition helix, resulting in thousands of DNA sequences uniquely targeted by ZFs.[28–31]

Because of their modularity and orthogonality, ZF tags provide an attractive capture chemistry for use in self-assembled protein microarrays.

Our strategy for the fabrication of self-assembled protein microarrays for SPRI measurements is outlined below (Figure 3.1.) We first designed and synthesized zinc finger fusion proteins (ZFPs), which consist of a ZF fused to a target protein by a helical linker. Each of these ZFPs has a unique ZF domain, which binds sequence-specifically to a 9 base-pair (bp) DNA sequence. We use this sequence specificity to drive self-assembly on-chip. One-pot IVTT is performed *ex situ* in a microcentrifuge tube containing plasmid DNAs encoding for each of the ZFPs to be arrayed. The resulting crude protein mixture is diluted and introduced to a dsDNA microarray via microfluidics. The ZFPs adsorb to their DNA targets on-chip via specific
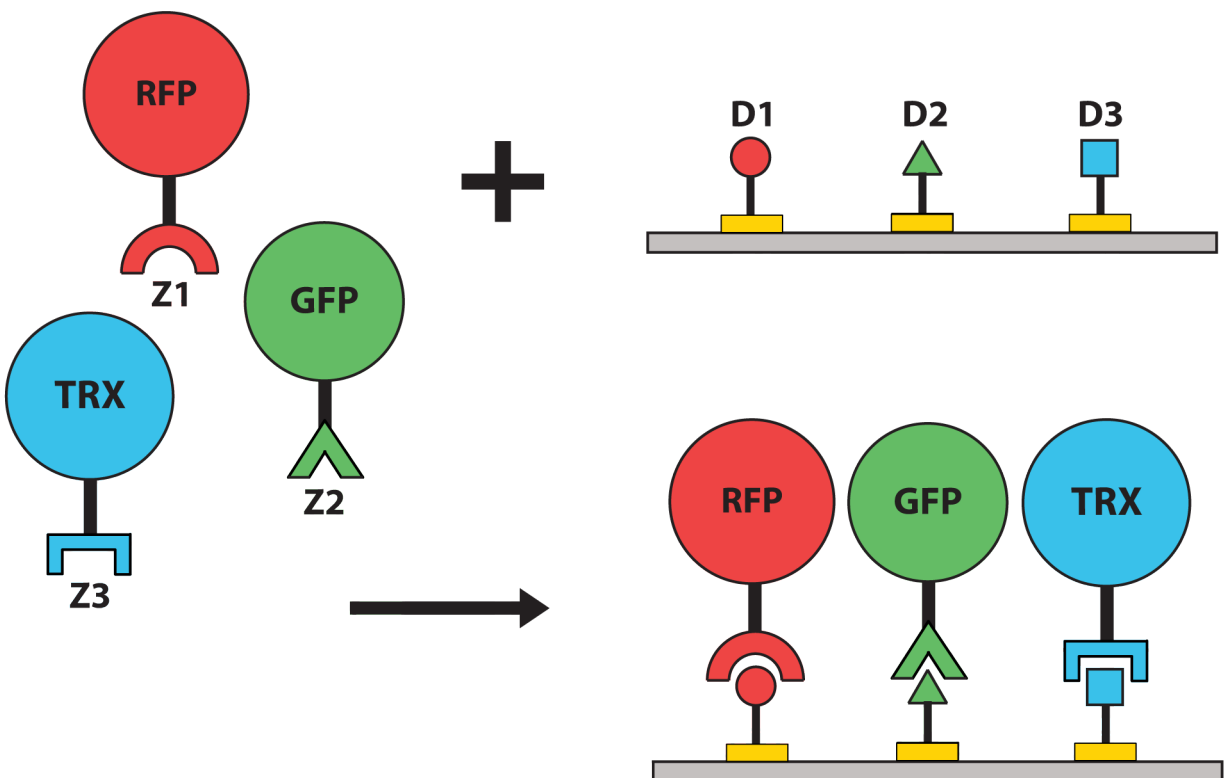
Figure 3.1: Self-Assembled Protein Microarray Strategy. To create a self-assembled protein microarray, each protein needs to have a unique capture tag (Z1, Z2, Z3), specific for a capture element on the surface (D1, D2, D3). Each of these capture chemistries must be orthogonal to one another and must not perturb protein function.

39

ZF/DNA interactions, resulting in a self-assembled protein microarray.

3.2 Experimental Considerations

3.2.1 Chemicals and Materials

All chemicals were purchased from Sigma-Aldrich and used without further purification unless otherwise specified. 11-mercatoundecamine (MUAM) was purchased from Dojindo. All DNAs were purchased from Integrated DNA Technologies (IDT) and purified by 7.5% PAGE. Polyclonal anti-GFP and anti-mCherry were purchased from Abcam. Nitrilotriacetic Acid (NTA) functionalized glass was purchased from ArrayIt. SF10 glass slides were purchased from Schott and plasma cleaned prior to vapor deposition of gold thin films. All water used was purified by a Milli-Q integral water purification system. Unless otherwise specified, all phosphate buffered saline (PBS) used is 100 mM Na_2HPO_4, 0.3 M NaCl, 5 mM $MgCl_2$, 1 mM EDTA, pH 7.4.

pET His6 GFP TEC LIC cloning vector and pET Biotin His6 mCherry LIC cloning vector were a gift from Scott Gradia (Addgene plasmid 29663 and 29722, respectively). PCR was performed using iProof HF Master Mix (Bio-Rad). Competent *E. coli* (5-alpha Competent *E. coli*) was purchased from New England Biolabs. IVTT kits (S30 T7 High-Yield Protein Expression System) were purchased from Promega. Fluorescence images were obtained using an Olympus IX-71 fluorescence microscope using an Andor Neo 5.5 sCMOS detector and a 100 W xenon-arc lamp light source. Both GFP and YFP fluorescence filter cube sets were purchased from ThorLabs. Dynabeads MyOne beads were purchased from Thermo-Fisher.

3.2.2 Zinc finger protein encoding DNA construction

Zinc finger fusion proteins were synthesized by ligation independent cloning (LIC). The following LIC linkers were designed to encode a helical peptide linker and DNA for vector annealing: Forward: 5'-TAC TTC CAA TCC AAT GCA GCT GAG GCA GCC GCT AAA GCG GAG GCG GCA GCA AAA GCC AAA AAA TCT AGA CCC GGG GAG-3'. Reverse: 5'-TTA TCC ACT TCC AAT GTT ATT TAA CTT CTT GGA TCC CCT CAG GTG-3'. These DNAs were ligated to the insert by PCR, and then purified using the QIAquick PCR purification kit (Qiagen). The purified insert + LIC linker was treated with T4 DNA polymerase (NEB) in the presence of dCTP and incubated at 37°C for 1 h, resulting in overhangs that are 15 nucleotides long. pET vectors encoding GFP and RFP were linearized by digestion using SspI, then treated with T4 DNA polymerase in the presence of dGTP in parallel with the insert DNA. The resulting solutions were used in annealing and transformation without further purification.

0.75 μL (5 fmol) of the digested vector and 4 μL (20 fmol) insert were mixed together and were incubated at room temperature for 5 min. Then, 1 μL of 25 mM EDTA was added to the mixture, followed by a second incubation period of 5 min at room temperature. This solution was used for transformation into competent *E. coli* without further purification. Annealed vectors were transformed into competent *E. coli* and plated onto LB agar with 40 μg/mL kanamycin for overnight growth at 37°C. LB media (5 mL) with 40 μg/mL kanamycin was inoculated with single colonies from these plates and allowed to grow overnight at 37°C in a shaking incubator. Plasmids from this solution were purified using the QIAprep Spin -Miniprep Kit (Qiagen) and quantified by Nanodrop.

3.2.3 Surface DNAs Used in This Study

The following DNAs and their complements are used for attachment to surfaces via p-Glu chemistry. ZF recognition sequences are in red.

D_0: NH$_2$-(CH$_2$)$_6$-5'-GGA CCG ATT GAC TTG ATA TAT AAA AAA AAA AAC ATT C-3'

D_1: NH$_2$-(CH$_2$)$_6$-5'-GGA CCG ATT GAC TTG ATA TAT AGC GTG GGC GAC ATT C-3'

D_2: NH$_2$-(CH$_2$)$_6$-5'-GGA CCG ATT GAC TTG ATA TAT AGG AGA TGG TAC ATT C-3'

3.2.4 Time Course Fluorescence Measurements

Multiplexed *in vitro* coupled transcription/translation was performed following the manufacturer's protocol for a 50 µL reaction and then diluted with water to a final volume of 65 µL to fill the fluorescence cuvette window. This mixture contained 500 ng of each plasmid DNAs for RFP-Z_1 and GFP-Z_2. The spectrofluorometer was blanked with PBS prior to data collection. Time course fluorescence measurements were taken over a period of 6 h, recording the emission intensity once every 10 seconds. Fluorometer settings limited experiments to single fluorophore measurements at a time. Therefore, two separate reactions were performed, monitoring real-time biosynthesis of RFP-Z_1 (λ_{ex} = 575 nm, λ_{em} = 610 nm) and GFP-Z_2 (λ_{ex} = 450 nm, λ_{em} = 510 nm) by fluorescence. Post-synthesis spectra were then measured to confirm the presence of both species in the final reaction mixture. All excitation and emission were measured with a 10 nm bandwidth, and the instrument sensitivity was set to 800 V.

3.2.5 IVTT Protein Synthesis

In vitro coupled transcription/translation (IVTT) was performed per the manufacturer's recommendation. The resulting protein mixtures were exchanged into ZF buffer by 3 kDa Amicon Ultra centrifugal filters (Millipore) before use.

3.2.6 FTIR Measurements of dsDNA Surfaces

A gold-coated microscope slide was created by vapor deposition of a 1 nm chromium adhesion layer followed by 100 nm of gold. This slide was then placed in a 1 mM ethanolic solution of MUAM and allowed to react at room temperature overnight. After this incubation period, the chip was washed with ethanol and water, then dried under N_2. A 500 mL solution of 2 mg/mL poly-L-glutamic acid (p-Glu) (MW 50-100k) in PBS and was electrostatically adsorbed to the amine surface by a 1 h incubation period at room temperature. The chip was then washed with water and dried under N_2. Prior to spotting on the p-Glu surface, DNA was annealed by heating and cooling. A solution of 3.2 μL, 1 mM 5'-amino-C_6-DNA (3.2 nmol) and 4.2 μL of 1 mM complementary DNA (4.2 nmol) was added to 2.6 μL of PBS. The reaction was performed with complementary DNA in excess to prevent the reaction of amino-ssDNA to the surface. The resulting mixture was then incubated at 95°C for 2 min then allowed to cool to room temperature and used in the following EDC/NHSS coupling chemistry: A 20 μL solution containing 75 mM EDC, 15 mM NHSS, and 160 μM dsDNA in PBS was added to gold-coated slide. A coverslip was added and the reaction was allowed to proceed at room temperature in a humidity chamber.

FTIR spectra were then collected using a Jasco FT/IR-4100 equipped with a Refractor 2 accessory (Harrick) and a liquid nitrogen cooled MCT detector (InfraRed).

3.2.7 On-Chip Fluorescence Measurements

NHS ester functionalized glass slides were photopatterned into a square grid by UV irradiation (260 nm, 400 W power from a mercury-xenon arc lamp) using a chromium-quartz mask for 1 h, producing a slide consisting of a pattern of NHS ester squares surrounded by a glass grid. After photopatterning, the slide was washed with water and dried under N_2. A 20 μL solution of 75 mM EDC, 15 mM NHSS, and 160 μM dsDNA in PBS was added to the photopatterned slide. A coverslip was added to disperse the solution and the chip was allowed to react for 12 h in a humidity chamber at room temperature. The coverslip was then removed and the slide was washed with PBS and dried under a stream of N_2. A 30 mL solution containing a 1:10 dilution of crude ZFP in ZF buffer (20 mM Tris, 50 mM KCl, 100 μM $Zn(NO_3)_2$, 1 mM $MgCl_2$) was added to the washed slide. The ZFPs were allowed to adsorb to the surface under a coverslip for 20 min at room temperature. After the incubation period, the coverslip was removed and the slide was washed gently by agitating in 5 mL ZF buffer (300 mM KCl, 0.01% Triton X-100) three times for 15 minutes each. The slide was then covered with 30 μL of ZF buffer and a coverslip for observation by fluorescence microscopy. All images were taken with a 10x objective and then processed and analyzed by Image J (National Institute of Health).

3.2.8 Magnetic Bead Functionalization

Dynabeads MyOne Carboxylic Acid magnetic beads were functionalized with D_0 for washing of IVTT reactions prior to SPRI experiments. 50 μL (0.5 mg) of beads were added to a 1.5 mL microcentrifuge tube. The beads were collected on the side of the tube using a neodymium magnet and the supernatant was removed. The beads were washed with 100 μL of MES buffer pH 5.0 by agitation for 30 s, and then collected for supernatant removal. 16.2 μL of

MES buffer and 1.8 μL of 500 μM single stranded amino D0 was added to the beads. The beads

were mixed by vortex and then were incubated at 25°C for 30 min. The beads were resuspended

in PBS and 2 μL of 10 mg/mL EDC was added. The reaction was allowed to proceed at 4°C for

14 h. After incubation, the beads were collected and the supernatant was removed. The beads

were resuspended in 50 μL PBS. The resulting single stranded D_0 beads were then annealed with

its complementary ssDNA; 50 μL of 40 μM complementary D_0 was added to the beads and the

mixture was heated to 95°C and then cooled to room temperature. The beads were then analyzed

by 2% agarose gel electrophoresis and visualized by SYBR Green I to estimate efficiency against

a standard. Based on these experiments, we estimate that 5 μM of dsD_0 was covalently attached

to the beads. These beads were then washed three times with PBS and used in crude ZFP

preparation without any further modification.

3.2.9 Preparation of Crude ZFPs for SPRI Analysis

After biosynthesis of ZFPs by IVTT, as described in section 3.2.4, crude ZFP mixtures

were washed with D_0 functionalized magnetic beads to remove any high-affinity nonspecific

DNA binders from the solution. To do this, 2 μL of crude ZFP was diluted into ZF Buffer + 300

mM KCl. This was added to 20 μL of D_0 functionalized magnetic beads and gently mixed for 1 h

at room temperature. The beads were collected and the supernatant was diluted into 1 mL of ZF

Buffer.

3.2.10 Preparation of DNA functionalized SPRI Chips

Functionalized SPRI chips were created using a procedure adapted from previous work

and similarly to section 3.2.6.[6] SPRI chips were placed in a 1 mM ethanolic solution of MUAM

and allowed to react at room temperature overnight. The chips were washed with ethanol and water, then dried under N_2. A 500 mL solution of 2 mg/mL p-Glu in PBS and was electrostatically adsorbed to the amine surface over a 1 h incubation period at room temperature. The chip was then washed with water and dried under N_2. Prior to spotting on the p-Glu surface, DNA was annealed by heating and cooling in the same manner as section 3.2.6. The resulting mixture was then incubated at 95°C for 2 min and allowed to cool to room temperature and used in the following EDC/NHSS coupling chemistry: A solution containing 75 mM EDC, 15 mM NHSS, and 160 μM dsDNA in PBS was spotted (5 μL) on the surface and allowed to react at room temperature in a humidity chamber overnight resulting in a dsDNA array. This array was used in SPRI experiments.

3.2.11 SPRI Measurements

Real-time SPRI measurements were obtained with an SPRimager instrument from GWC Technologies as described previously.[32] All microfluidics components were sonicated in ethanol for 5 min, then washed with ethanol and then water followed by drying under a N_2 stream. DNA functionalized SPRI chips were placed in the SPRI setup after DNA attachment and the SPRI chips were washed with ZF Buffer using the instrument's microfluidics for 5 min. A 4:1000 solution of 3 kDa filtered protein mixture in ZF buffer was introduced to the SPRI chip and recycled over 20 minutes while binding data was collected.

3.3 Results and Discussion

3.3.1 Design and Biosynthesis of ZFPs

Two exemplary ZFPs were used in this initial study: mCherry-Z_1 (RFP-Z_1) and green fluorescent protein-Z_2 (GFP-Z_2). As illustrated in Figure 3.2, each ZFP consists of a target protein, a 13 residue helical linker,[33,34] and a 3-domain zinc finger motif capable of specific binding to a 9 bp dsDNA sequence. Each zinc finger is selective for one of the DNAs in mentioned in section 3.2.3. Z_1 and Z_2 bind to D_1 and D_2 respectively. D_0 is used as a negative control.[35] Z_1 is a zinc finger domain belonging to the widely studied Zif-268,[22–24,27] while Z_2 is a domain derived using the CoDA method for zinc finger engineering.[31] DNAs encoding each ZF were inserted into target protein cloning vectors *via* ligation-independent cloning and confirmed by Sanger sequencing. Both proteins were synthesized using IVTT. The resulting proteins were characterized by SDS-PAGE (not shown) and also in real time with fluorescence spectroscopy.

First, to show that IVTT of the two proteins is possible in a single 50 μL reaction, *in vitro* synthesis of ZFPs was monitored by time course fluorescence measurements. By observing the fluorescence of the target protein domains for both these ZFPs over time, we confirm the successful biosynthesis and folding of these fusion proteins. Simultaneous synthesis of RFP-Z1 and GFP-Z2 was performed over 6 hours; results from two separate experiments are shown in Figure 3.3. Each experiment contained both DNAs encoding RFP-Z1 and GFP-Z2. Constraints in the time course fluorescence measurements limited us to measuring the fluorescence of a single protein per experiment in this multiplexed IVTT. Post-synthesis spectra were also measured, to verify that both species were present (not shown).
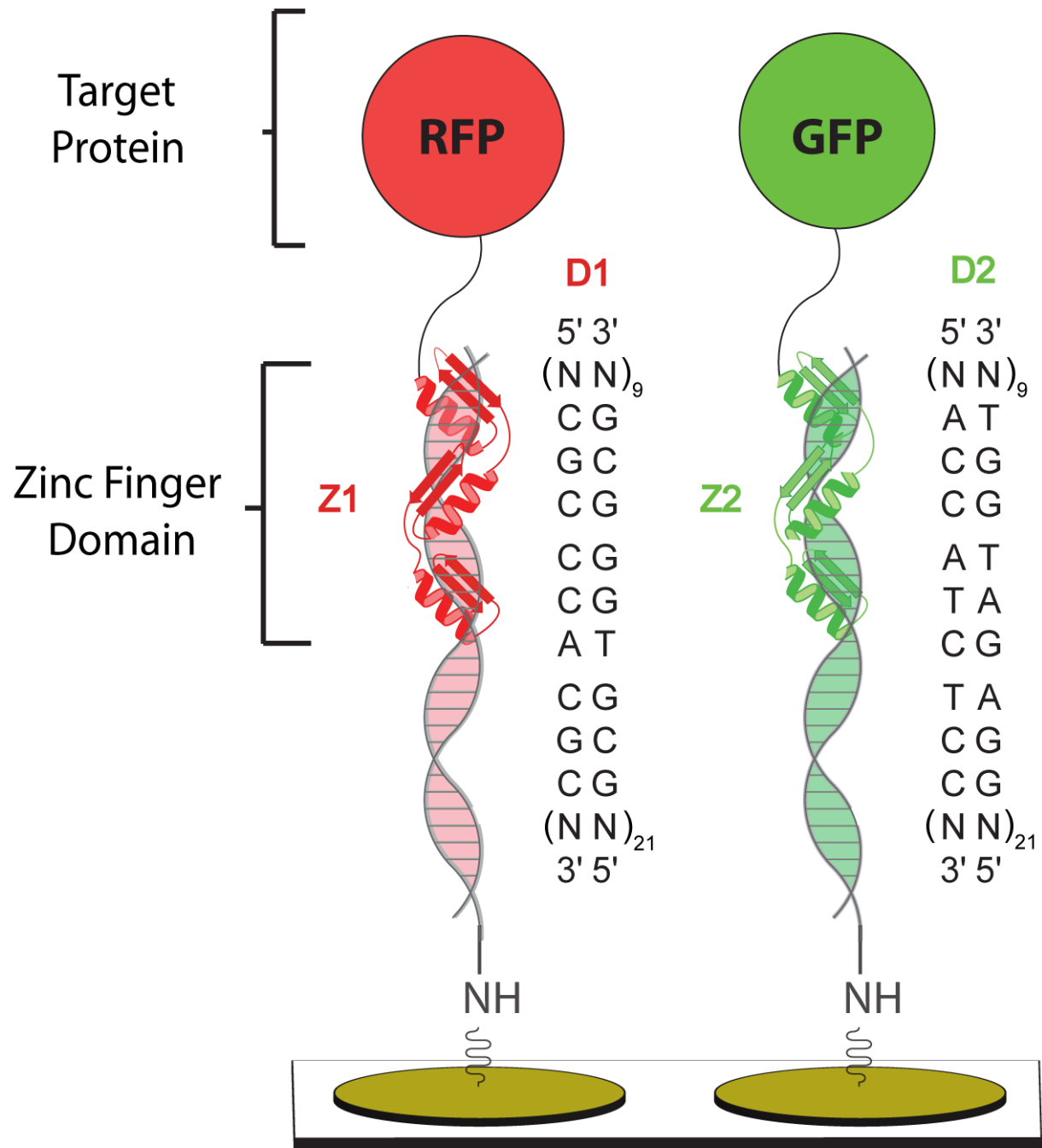
Figure 3.2 Zinc-Finger Mediated Self-Assembled Protein Microarrays. A dsDNA array is created on an SPRI chip using poly-L-glutamic acid coupling chemistry. Each dsDNA includes a unique 9 bp ZF binding sequence. ZFPs are introduced to the array and adsorb specifically to their dsDNA partner on chip, resulting in a self-assembled protein microarray.

As shown in Figure 3.3 we verify that both proteins are capable of being synthesized simultaneously in the same reaction. We attribute the initial drop in fluorescence to the consumption of fluorescent reagents (FADH, NADH) present in the IVTT solution necessary for protein synthesis. The slower fluorescence increase of RFP-Z_1 compared to GFP-Z_2 is indicative of its longer maturation time, compared to the "superfolding" GFP.[36] Further, we note that the final fluorescence of RFP-Z1 is 60% higher than its initial fluorescence, whereas GFP-Z_2 signal is 600% higher. This difference is attributed to the higher quantum yield of GFP over RFP as previously reported.[37] We estimate the total concentration of target protein synthesized to be 300
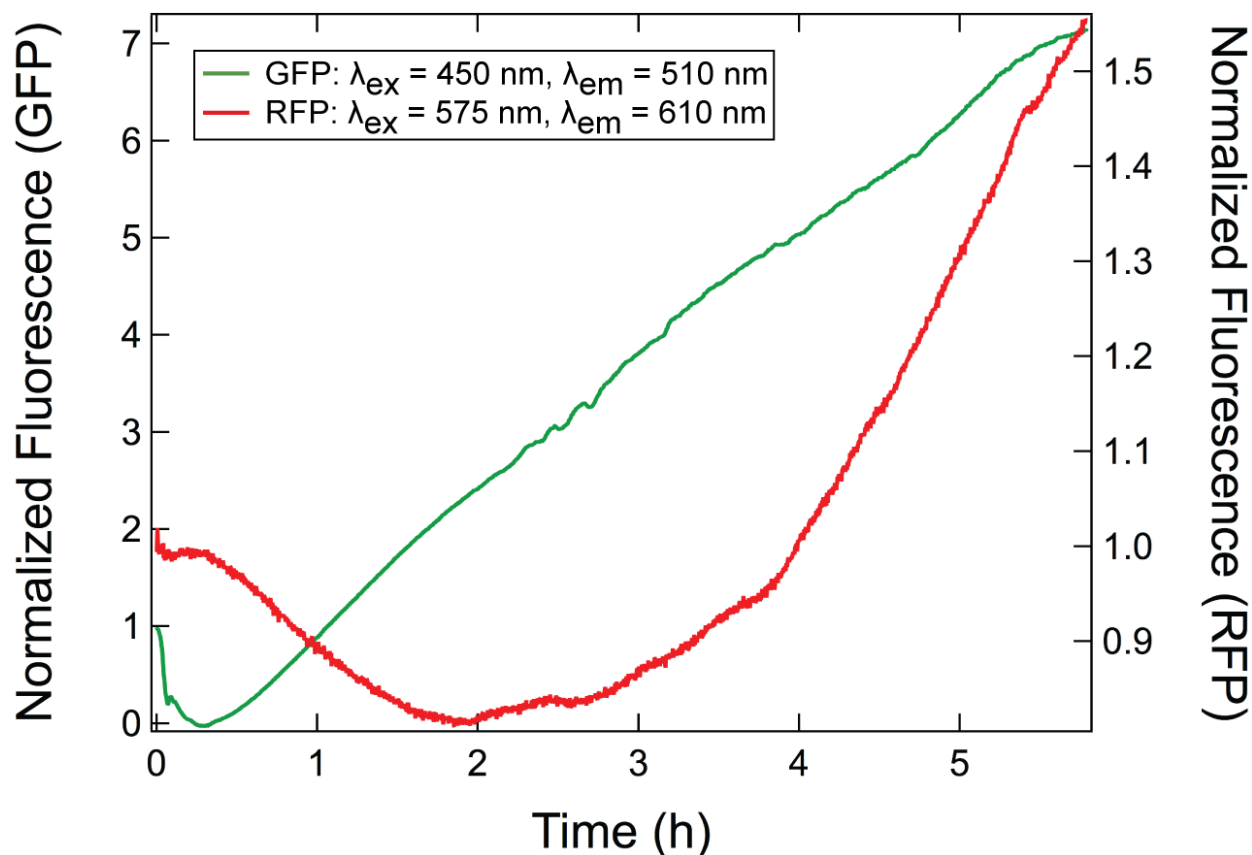
Figure 3.3 Simultaneous syntheses of RFP-Z1 and GFP-Z2 was monitored over time via fluorescence. Because mCherry is a weaker fluorophore, it is shown at 10x in this graph to scale with GFP.

nM measured by absorbance at 280 nm of a Ni^{II}-NTA purified sample. This is a sufficient amount of protein for the surface capture of ZFPs since the K_d's of three-finger C_2H_2 zinc fingers conservatively range between 1 and 10 nM.[29] These data confirms that multiple proteins can be synthesized via single-batch IVTT at a concentration suitable for immobilization onto dsDNA arrays.

3.3.2 Fabrication and Characterization of dsDNA Surfaces

Double stranded DNA (dsDNA) surfaces were created using poly-L-glutamic acid (p-Glu) chemistry as described in the experimental section. We characterized these surfaces via FTIR as shown in Figure 3.4. Peaks at 1666 cm^{-1} (amide I) and 1569-1522 cm^{-1} (amide II) indicate the presence of p-Glu as described previously,[6] while peaks characteristic of DNA at 1642 cm^{-1}(amide I), at 1569-1522 cm^{-1}(amide II), and at 1265 cm^{-1} and 1046 cm^{-1} (phosphate antisymmetric and symmetric, respectively) are also present.[38] We also observe peaks at 1730 cm^{-1} and 1145 cm^{-1}, which are characteristic of the acid carbonyl and C-O stretches respectively. This FTIR data indicates that DNA is attached to the surface. However, the presence acid carbonyl peaks shows a significant amount of unreacted carboxylic acid on the surface indicating unreacted p-Glu to either DNA or the MUAM monolayer.

To test the functionality of our dsDNA surfaces for SPRI, we produced a dsDNA microarray using the same p-Glu chemistry as used for FTIR and then introduced the array to single-stranded DNA binding protein (SSB). Upon introduction of 124 nM SSB in PBS to a multicomponent dsDNA/ssDNA functionalized microarray (Figure 3.5), we observed minimal adsorption to elements containing dsDNA (0.16 ± 0.27 $\Delta\%R$), while we see larger adsorption
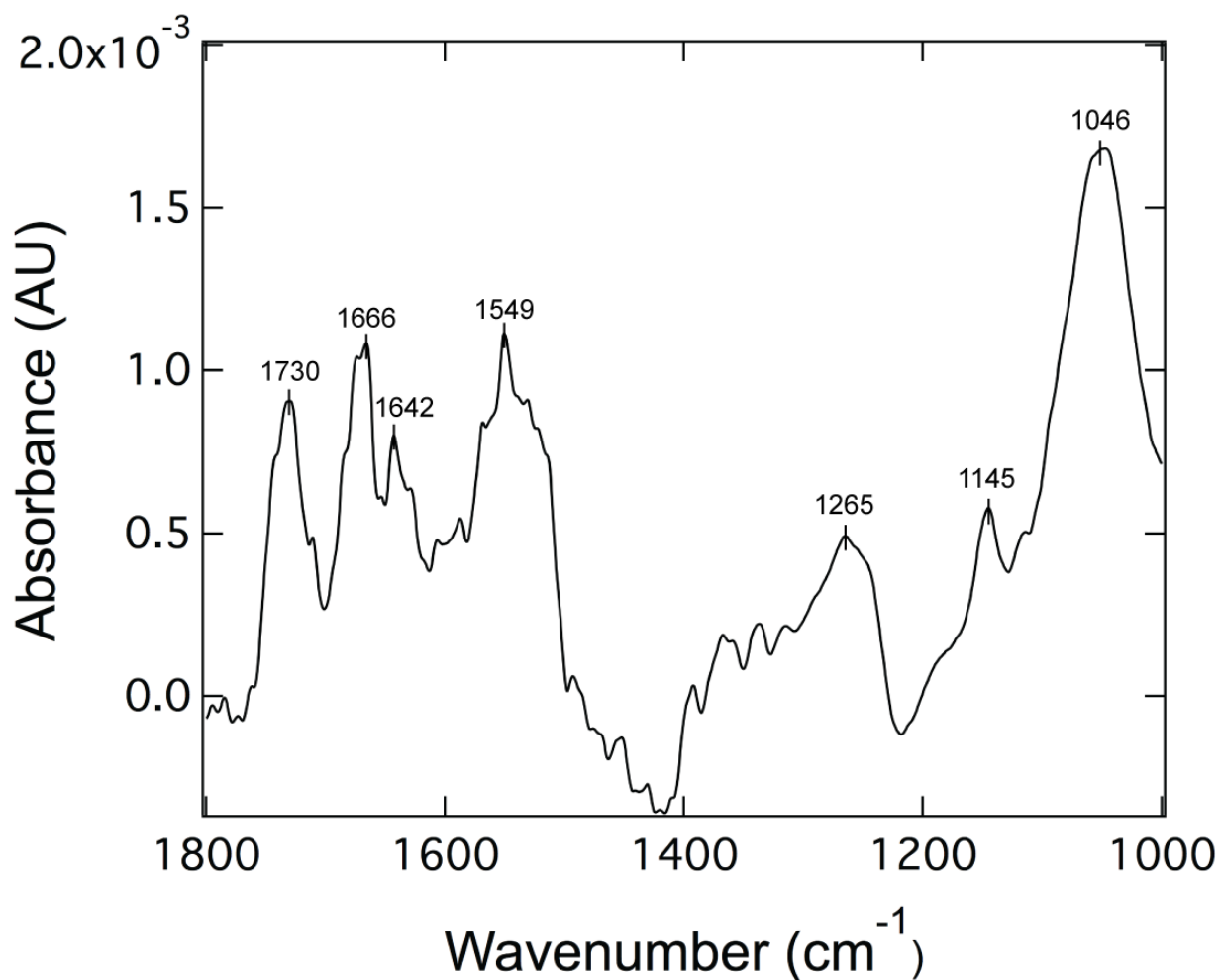
Figure 3.4: Grazing Angle Reflectance FTIR of dsDNA Surfaces. Double-stranded DNA was attached to a gold thin-film surface using p-Glu chemistry. Peaks and assignments are outlined in Table 3.1

Table 3.1 Frequencies of FTIR Spectrum Shown in Figure 3.3

Wavenumber (cm^{-1})	Assignment
1731	C=O (acid)
1666	Amide I (p-Glu)
1642	Amide I (DNA)
1569-1522	Amide II (p-Glu/DNA)
1265	Phosphate antisymmetric (DNA)
1145	C-O (p-Glu)
1046	Phosphate symmetric (DNA)

signal (5.21 ± 0.68 Δ%R) for a single stranded DNA control. Since SSB has been shown to not adsorb to dsDNA elements[6] and SSB adsorption to a bare p-Glu surface yields a Δ%R comparable to ssDNA elements (data not shown), we predict that the relatively low SPRI signal observed from dsDNA elements in this experiment is due to the presence of dsDNA on the surface.

This SPRI data in combination with the FTIR data shown in Figure 3.4 provide strong evidence for the formation of functional dsDNA surfaces for use in this study.
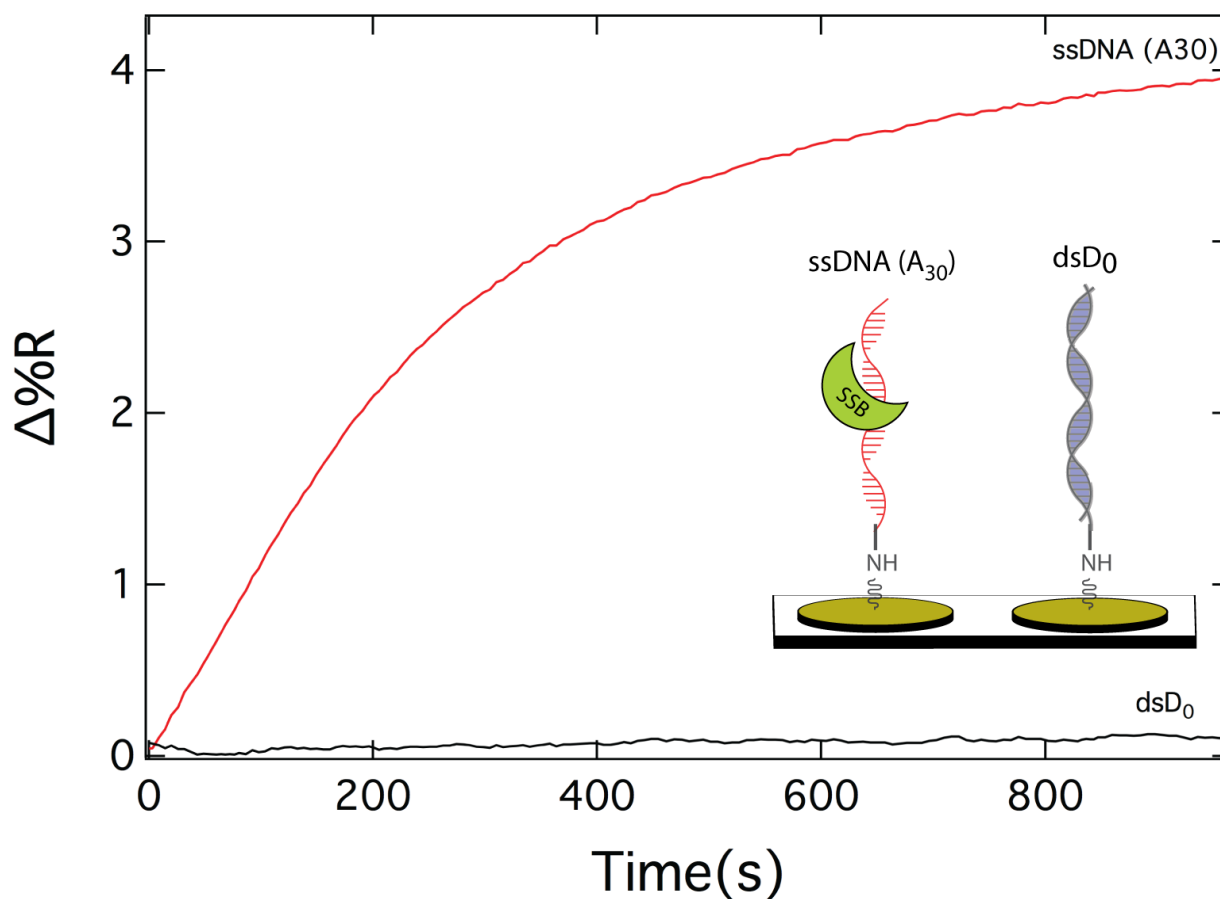
Figure 3.5: SPRI of SSB adsorption to a DNA surface. SSB was exposed to a DNA surface in order to confirm surface fidelity. SSB adsorbs to both ssDNA and to a bare p-glu surface, but does not adsorb to dsDNA. After exposure of a DNA functionalized SPRI chip to 124 nM SSB, we observe adsorption of SSB to ssDNA elements (5.21 ± 0.68 Δ %R) while a small amount of adsorption (0.16 ± 0.27 Δ%R) is observed on dsDNA elements.

3.3.3 On-Chip Fluorescence of ZFP Adsorption to dsDNA Surfaces

ZFPs were examined for specific binding to their surface-attached dsDNAs, while maintaining target protein functionality. Because our ZFPs are also inherently fluorescent, we tested ZFP functionality by fluorescence microscopy. To do this, NHS-ester functionalized glass slides were photopatterned by UV irradiation to create a pattern of 90 μm squares, and then amino dsDNA was attached to the surface using EDC/NHSS coupling chemistry described previously.[6,13]

To observe ZFP adsorption to this patterned dsDNA surface, a 15 nM crude IVTT solution containing either ZFP was introduced to its corresponding dsDNA surface and to a D_0 control surface. After a brief incubation period and washing, fluorescence of the ZFPs was observed by microscopy as shown in Figure 3.6. Upon introducing RFP-Z_1 to a D_1 surface, fluorescence (λ_{ex} = 562 nm, λ_{em} = 641 nm) was observed in the expected square pattern where DNA is attached. This fluorescence persists even after multiple washes with ZF buffer (300 mM KCl, 0.01% triton X-100). Similarly, introducing RFP-Z_1 to a D_0 control surface yields the same patterned fluorescence as the D_1 surface initially; however, washing of this surface decreases RFP-Z_1 fluorescence to the values shown in Figure 3.6. These data show that even though RFP-Z_1 adsorbs to D_0 nonspecifically, its affinity to its target sequence is much higher. Overall, we found that D_1 surfaces exhibit 10 times more fluorescence than D_0 surfaces after these washing steps.

These experiments were repeated with GFP-Z_2, but with its binding partner D_2 attached to the photopatterned surface and we observed persistent, patterned fluorescence (λ_{ex} = 445 nm, λ_{em} = 510 nm) after multiple washing steps. Identical treatment of patterned D_0 surfaces exposed to GFP-Z_2 resulted in a large decrease in fluorescence to levels shown in SI Figure 3A.1.
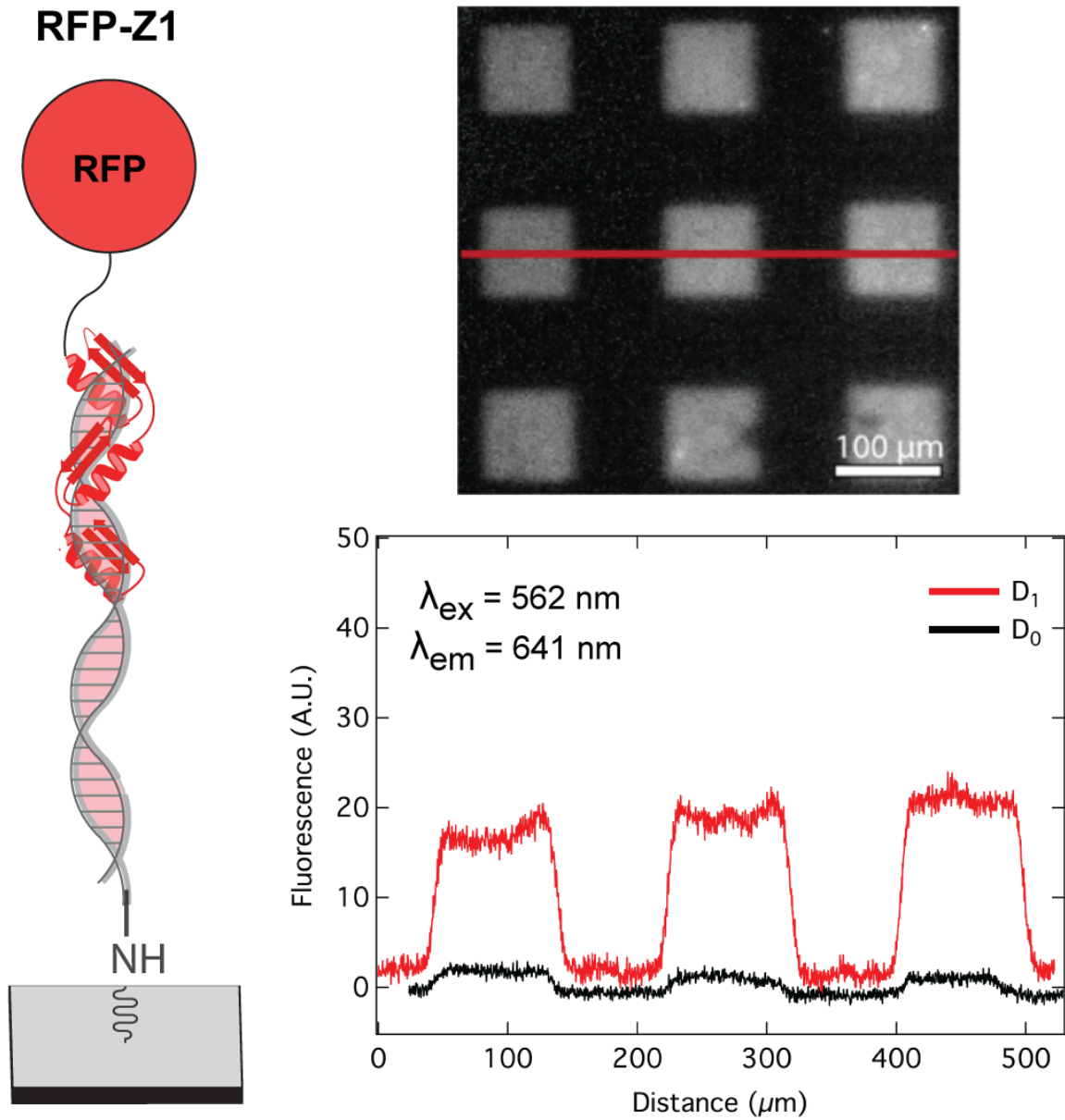
Figure 3.6: Fluorescence Microscopy of RFP-Z_1 Adsorption to dsDNA surfaces. Adsorption of unpurified RFP-Z_1 to dsDNA surfaces was measured by fluorescence microscopy. These studies enable us to test the functionality of both the ZF and RFP domains of the ZFP. Fluorescence from adsorption to a D_0 was also measured, though the image is not shown. The images were integrated and plotted, showing 10-fold more fluorescence for the D_1 surface over the D_0 surface.

Overall, we observe that D_2 surfaces exhibit 4 times more fluorescence than D_0 surfaces. We attribute this higher background in GFP-Z_2 experiments to non-specific adsorption of GFP-Z_2 that is not easily washed away. This suggests that GFP-Z_2 has a higher affinity to D_0 than RFP-Z_1.

In these experiments, we observed that high initial fluorescence indicating ZFP adsorption to D_0 surfaces that can be washed away, suggesting weak, non-specific affinity for our ZFPs to D_0. These observations are consistent with the mechanisms of DNA binding proteins, described by others as a two-step process with an initial non-specific DNA binding step, followed by a target sequence "searching" step, either by "sliding," "hopping," or "intersegmental transfer" along a DNA.[39,40] Since D_0 does not include the binding sequences for either ZFP, we predict that this initial non-specific adsorption is due to this initial DNA binding step, while the persistent fluorescence is a result of the ZFP bound to its target DNA sequence.

These experiments demonstrate that the zinc finger domains in both ZFPs are functional and selective for their DNA partners on surfaces against a D_0 control. Furthermore, adsorption seems to occur in a manner that is consistent with previous mechanistic studies of DNA binding proteins. These experiments demonstrate the functionality of the fluorescent domain of each ZFP, indicating that proteins fused to ZFs in this methodology are correctly expressed and folded, which is essential for a successful protein microarray methodology.

3.3.4 SPRI of ZFP Adsorption onto DNA Microarrays

After confirming the functionality of ZFPs to adsorb to their target DNAs specifically on-chip while maintaining target protein functionality, we wanted to study the ability of our ZFPs to selectively self-assemble on multicomponent DNA arrays. We began by introducing them to

two-component DNA microarrays consisting of immobilized D_0 and either D_1 or D_2. Using microfluidics, we then introduced ZFP IVTT reactions to the array and measured adsorption by SPRI. Since SPRI is a technique that is sensitive to any surface adsorption, we took steps to remove non-specific DNA binders from the crude IVTT reaction. To do this, we treated the crude IVTT mixtures with D_0 functionalized magnetic beads. The resulting washed IVTT solutions were then introduced to these two-component DNA microarrays for analysis by SPRI.

As shown in Figure 3.7, we see that both RFP-Z_1 and GFP-Z_2 adsorb preferentially to both D_1 and D_2, respectively, over D_0. When RFP-Z_1 is introduced to a D_1/D_0 array, we observe adsorption to D_1 of 1.36 ± 0.12 $\Delta\%R$ over adsorption to D_0 (Figure 3.7a). Similar results are observed when GFP-Z_2 is introduced to a D_2/D_0 surface. In this case, we observe adsorption to D_2 of 1.28 ± 0.72 $\Delta\%R$ over D_0 (Figure 3.7b). We attribute this difference to the specific adsorption of ZFPs to their respective DNA targets. The $\Delta\%Rs$ obtained here are similar, which is consistent with the similar size and concentration of both ZFPs (43.8 kDa for RFP-Z_1 and 42.2 kDa for GFP-Z_2). We also observe a difference in kinetics for the adsorption of RFP-Z_1 and GFP-Z_2 to their respective DNA targets. RFP-Z_1 reaches saturation after 1200 s while GFP-Z_2 reaches saturation after only 700 s. We hypothesize that this difference is due to a difference in K_d, but further kinetics studies will need to be performed to confirm this hypothesis.

We also report that we observe significant adsorption to D_0, with this adsorption accounting for approximately 80% of our total SPR signal in both experiments. We attribute this signal to the non-specific adsorption of proteins from the IVTT reaction to the DNA surface that were not removed by our prewashing steps. Since the IVTT reaction contains proteins that rely on initial non-specific adsorption to nucleic acids to perform the chemistry
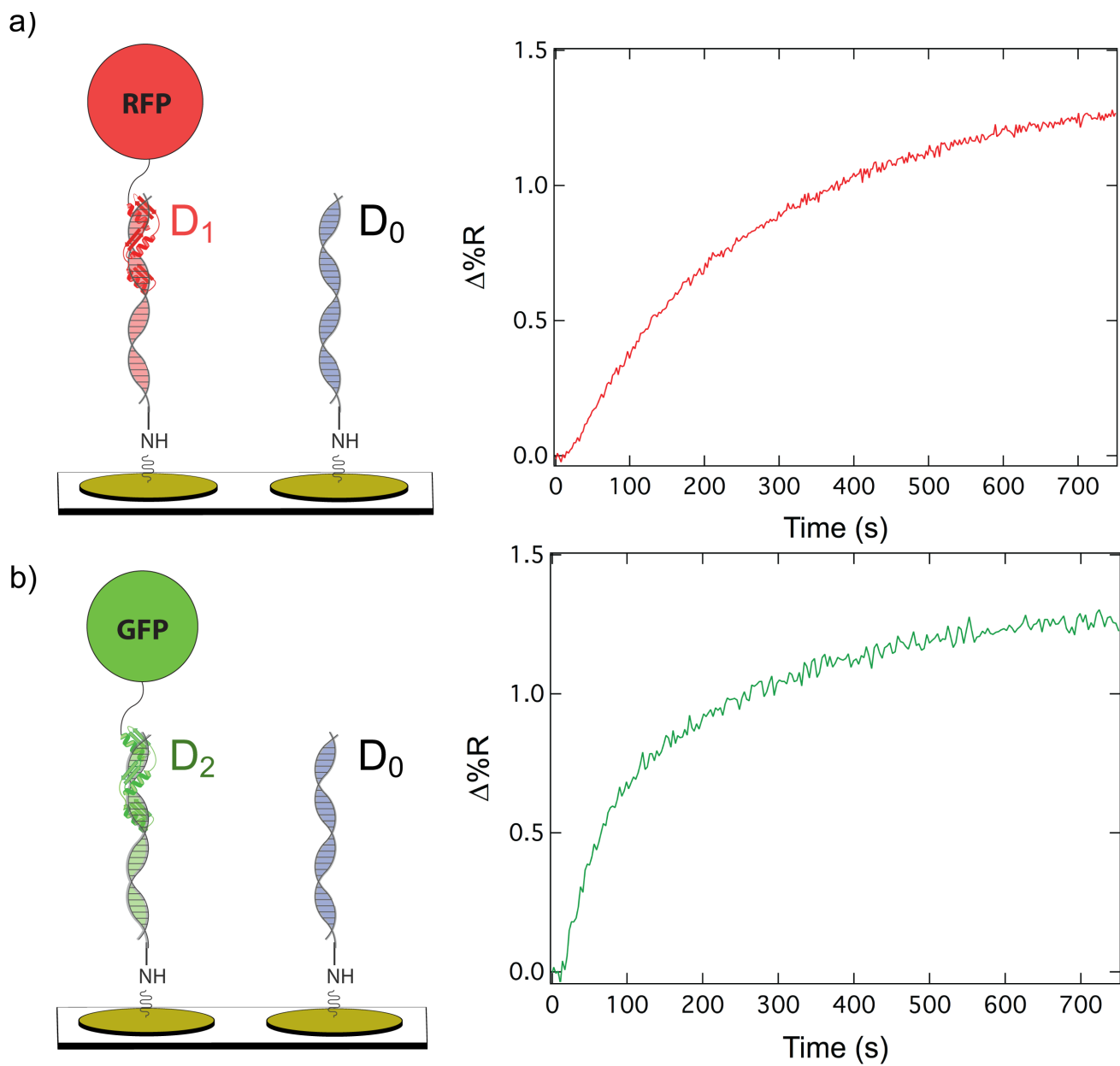
Figure 3.7: SPRI of adsorption of zinc fingers to 2-component DNA microarrays. (a) Adsorption of RFP-Z_1 to an array of D_1 and D_0. (b) Adsorption of GFP-Z_2 to an array of D_2 and D_0. Adsorption of these ZFPs showed preferential adsorption to the respective DNAs over D_0 by approximately 1.3 $\Delta\%R$.

essential for protein synthesis, we suspect that these proteins are the cause of the observed non-specific adsorption to all surface sequences. Though steps were taken to reduce non-specific adsorption, additional steps must be taken to perturb the effects of these proteins.

Overall, these SPRI experiments complement the fluorescence data presented in the previous section, showing that our ZFPs adsorb to their target DNAs on-chip. Fluorescence experiments show specific ZFP adsorption to DNA surfaces, however SPRI experiments reveal a significant amount of non-specific adsorption of molecules in the IVTT mix that were unobservable in our on-chip fluorescence experiments. This provides an interesting perspective into current fluorescence-based IVTT protein microarray fabrication methodologies, where these non-specific binding may be present, but the effects on the array fidelity are not yet known.

3.4 Conclusions

In this chapter, we have shown that zinc finger affinity to DNA is a promising capture chemistry for use in self-assembled protein microarrays. Analysis by SPRI shows that zinc fingers fused to a protein target are able to find their DNA binding partners on a surface to create protein microarrays. Compared to other protein microarray fabrication methods, this method allows for protein synthesis off-chip, enabling the production of much larger proteins while also decreasing the volume of crude IVTT solution required compared to our previous methods.

Though great strides have been achieved in this chapter toward self-assembled protein microarrays, we must recognize that reducing non-specific adsorption of proteins to surfaces is of upmost importance in creating an SPRI biosensor in the future. The development of new surface attachment chemistries to try to minimize these interactions will be explored as well as the implementation of more effective washing steps. The potential of batch purification via a

universal tag off-chip prior to introduction on-chip will also be assessed. The chemistry developed in this chapter will also be used in other endeavors within the Corn group, namely in regiospecific protein display.

3.5 Acknowledgements

3.6 References

(1) Duarte, J. G.; Blackburn, J. M. Advances in the Development of Human Protein Microarrays. *Expert Rev. Proteomics* **2017**, *14* (7), 627–641.

(2) Moore, C. D.; Ajala, O. Z.; Zhu, H. Applications in High-Content Functional Protein Microarrays. *Curr. Opin. Chem. Biol.* **2016**, *30* (Supplement C), 21–27.

(3) Emili, A. Q.; Cagney, G. Large-Scale Functional Analysis Using Peptide or Protein Arrays. *Nat. Biotechnol.* **2000**, *18* (4), 393–397.

(4) Kingsmore, S. F. Multiplexed Protein Measurement: Technologies and Applications of Protein and Antibody Arrays. *Nat. Rev. Drug Discov.* **2006**, *5* (4), 310–321.

(5) Wilson, D. S.; Nock, S. Recent Developments in Protein Microarray Technology. *Angew. Chem. Int. Ed.* **2003**, *42* (5), 494–500.

(6) Chen, Y.; Nguyen, A.; Niu, L.; Corn, R. M. Fabrication of DNA Microarrays with Poly(l-Glutamic Acid) Monolayers on Gold Substrates for SPR Imaging Measurements. *Langmuir* **2009**, *25* (9), 5054–5060.

(7) Pirrung, M. C. How to Make a DNA Chip. *Angew. Chem. Int. Ed.* **2002**, *41* (8), 1276–1289.

(8) Singh, P. SPR Biosensors: Historical Perspectives and Current Challenges. *Sens. Actuators B Chem.* **2016**, *229*, 110–130.

(9) Manuel, G.; Lupták, A.; Corn, R. M. A Microwell–Printing Fabrication Strategy for the On-Chip Templated Biosynthesis of Protein Microarrays for Surface Plasmon Resonance Imaging. *J. Phys. Chem. C* **2016**.

(10) MacBeath, G.; Schreiber, S. L. Printing Proteins as Microarrays for High-Throughput Function Determination. *Science* **2000**, *289* (5485), 1760–1763.

(11) Joos, T. O.; Schrenk, M.; Höpfl, P.; Kröger, K.; Chowdhury, U.; Stoll, D.; Schörner, D.; Dürr, M.; Herick, K.; Rupp, S.; et al. A Microarray Enzyme-Linked Immunosorbent Assay for Autoimmune Diagnostics. *ELECTROPHORESIS* **2000**, *21* (13), 2641–2650.

(12) Afanassiev, V.; Hanemann, V.; Wölfl, S. Preparation of DNA and Protein Micro Arrays on Glass Slides Coated with an Agarose Film. *Nucleic Acids Res.* **2000**, *28* (12), e66.

(13) Seefeld, T. H.; Halpern, A. R.; Corn, R. M. On-Chip Synthesis of Protein Microarrays from DNA Microarrays via Coupled In Vitro Transcription and Translation for Surface Plasmon Resonance Imaging Biosensor Applications. *J. Am. Chem. Soc.* **2012**, *134* (30), 12358–12361.

(14) Yu, X.; LaBaer, J. High-Throughput Identification of Proteins with AMPylation Using Self-Assembled Human Protein (NAPPA) Microarrays. *Nat. Protoc.* **2015**, *10* (5), 756–767.

(15) Ramachandran, N.; Raphael, J. V.; Hainsworth, E.; Demirkan, G.; Fuentes, M. G.; Rolfs, A.; Hu, Y.; LaBaer, J. Next-Generation High-Density Self-Assembling Functional Protein Arrays. *Nat. Methods* **2008**, *5* (6), 535–538.

(16) Ramachandran, N.; Hainsworth, E.; Bhullar, B.; Eisenstein, S.; Rosen, B.; Lau, A. Y.; Walter, J. C.; LaBaer, J. Self-Assembling Protein Microarrays. *Science* **2004**, *305* (5680), 86–90.

(17) Olia, A. S.; Barker, K.; McCullough, C. E.; Tang, H.-Y.; Speicher, D. W.; Qiu, J.; LaBaer, J.; Marmorstein, R. Nonenzymatic Protein Acetylation Detected by NAPPA Protein Arrays. *ACS Chem. Biol.* **2015**, *10* (9), 2034–2047.

(18) He, M.; Stoevesandt, O.; Palmer, E. A.; Khan, F.; Ericsson, O.; Taussig, M. J. Printing Protein Arrays from DNA Arrays. *Nat. Methods* **2008**, *5* (2), 175–177.

(19) He, M.; Taussig, M. J. Single Step Generation of Protein Arrays from DNA by Cell-Free Expression and in Situ Immobilisation (PISA Method). *Nucleic Acids Res.* **2001**, *29* (15), e73.

(20) Tom, J. K.; Dotsey, E. Y.; Wong, H. Y.; Stutts, L.; Moore, T.; Davies, D. H.; Felgner, P. L.; Esser-Kahn, A. P. Modulation of Innate Immune Responses via Covalently Linked TLR Agonists. *ACS Cent. Sci.* **2015**, *1* (8), 439–448.

(21) Vaquerizas, J. M.; Kummerfeld, S. K.; Teichmann, S. A.; Luscombe, N. M. A Census of Human Transcription Factors: Function, Expression and Evolution. *Nat. Rev. Genet.* **2009**, *10* (4), nrg2538.

(22) Christy, B.; Nathans, D. DNA Binding Site of the Growth Factor-Inducible Protein Zif268. *Proc. Natl. Acad. Sci.* **1989**, *86* (22), 8737–8741.

(23) Elrod-Erickson, M.; Rould, M. A.; Nekludova, L.; Pabo, C. O. Zif268 protein–DNA Complex Refined at 1.6å: A Model System for Understanding Zinc finger–DNA Interactions. *Structure* **1996**, *4* (10), 1171–1180.

(24) Elrod-Erickson, M.; Benson, T. E.; Pabo, C. O. High-Resolution Structures of Variant Zif268–DNA Complexes: Implications for Understanding Zinc finger–DNA Recognition. *Structure* **1998**, *6* (4), 451–464.

(25) Pavletich, N. P.; Pabo, C. O. Zinc Finger-DNA Recognition: Crystal Structure of a Zif268-DNA Complex at 2.1 A. *Science* **1991**, *252* (5007), 809–817.

(26) Wolfe, S. A.; Grant, R. A.; Elrod-Erickson, M.; Pabo, C. O. Beyond the "Recognition Code": Structures of Two Cys2His2 Zinc Finger/TATA Box Complexes. *Structure* **2001**, *9* (8), 717–723.

(27) Swirnoff, A. H.; Milbrandt, J. DNA-Binding Specificity of NGFI-A and Related Zinc Finger Transcription Factors. *Mol. Cell. Biol.* **1995**, *15* (4), 2275–2287.

(28) Kim, J.-S.; Pabo, C. O. Getting a Handhold on DNA: Design of Poly-Zinc Finger Proteins with Femtomolar Dissociation Constants. *Proc. Natl. Acad. Sci.* **1998**, *95* (6), 2812–2817.

(29) Beerli, R. R.; Segal, D. J.; Dreier, B.; Barbas, C. F. Toward Controlling Gene Expression at Will: Specific Regulation of the erbB-2/HER-2 Promoter by Using Polydactyl Zinc Finger Proteins Constructed from Modular Building Blocks. *Proc. Natl. Acad. Sci.* **1998**, *95* (25), 14628–14633.

(30) Lam, K. N.; van Bakel, H.; Cote, A. G.; van der Ven, A.; Hughes, T. R. Sequence Specificity Is Obtained from the Majority of Modular C2H2 Zinc-Finger Arrays. *Nucleic Acids Res.* **2011**, *39* (11), 4680–4690.

(31) Sander, J. D.; Dahlborg, E. J.; Goodwin, M. J.; Cade, L.; Zhang, F.; Cifuentes, D.; Curtin, S. J.; Blackburn, J. S.; Thibodeau-Beganny, S.; Qi, Y.; et al. Selection-Free Zinc-Finger-Nuclease Engineering by Context-Dependent Assembly (CoDA). *Nat. Methods* **2011**, *8* (1), 67–69.

(32) Lee, H. J.; Nedelkov, D.; Corn, R. M. Surface Plasmon Resonance Imaging Measurements of Antibody Arrays for the Multiplexed Detection of Low Molecular Weight Protein Biomarkers. *Anal. Chem.* **2006**, *78* (18), 6504–6510.

(33) Marqusee, S.; Baldwin, R. L. Helix Stabilization by Glu-...Lys+ Salt Bridges in Short Peptides of de Novo Design. *Proc. Natl. Acad. Sci.* **1987**, *84* (24), 8898–8902.

(34) Arai, R.; Ueda, H.; Kitayama, A.; Kamiya, N.; Nagamune, T. Design of the Linkers Which Effectively Separate Domains of a Bifunctional Fusion Protein. *Protein Eng.* **2001**, *14* (8), 529–532.

(35) Bulyk, M. L.; Huang, X.; Choo, Y.; Church, G. M. Exploring the DNA-Binding Specificities of Zinc Fingers with DNA Microarrays. *Proc. Natl. Acad. Sci.* **2001**, *98* (13), 7158–7163.

(36) Pédelacq, J.-D.; Cabantous, S.; Tran, T.; Terwilliger, T. C.; Waldo, G. S. Engineering and Characterization of a Superfolder Green Fluorescent Protein. *Nat. Biotechnol.* **2006**, *24* (1), 79.

(37) Shaner, N. C.; Steinbach, P. A.; Tsien, R. Y. A Guide to Choosing Fluorescent Proteins. *Nat. Methods* **2005**, *2* (12), 905.

(38) Mello, M. L. S.; Vidal, B. C. Changes in the Infrared Microspectroscopic Characteristics of DNA Caused by Cationic Elements, Different Base Richness and Single-Stranded Form. *PLOS ONE* **2012**, *7* (8), e43169.

(39) Halford, S. E.; Marko, J. F. How Do Site-specific DNA-binding Proteins Find Their Targets? *Nucleic Acids Res.* **2004**, *32* (10), 3040–3052.

(40) Marcovitz, A.; Levy, Y. Frustration in protein–DNA Binding Influences Conformational Switching and Target Search Kinetics. *Proc. Natl. Acad. Sci.* **2011**, *108* (44), 17957–17962.

Appendix A

Supplementary Information for Chapter 3
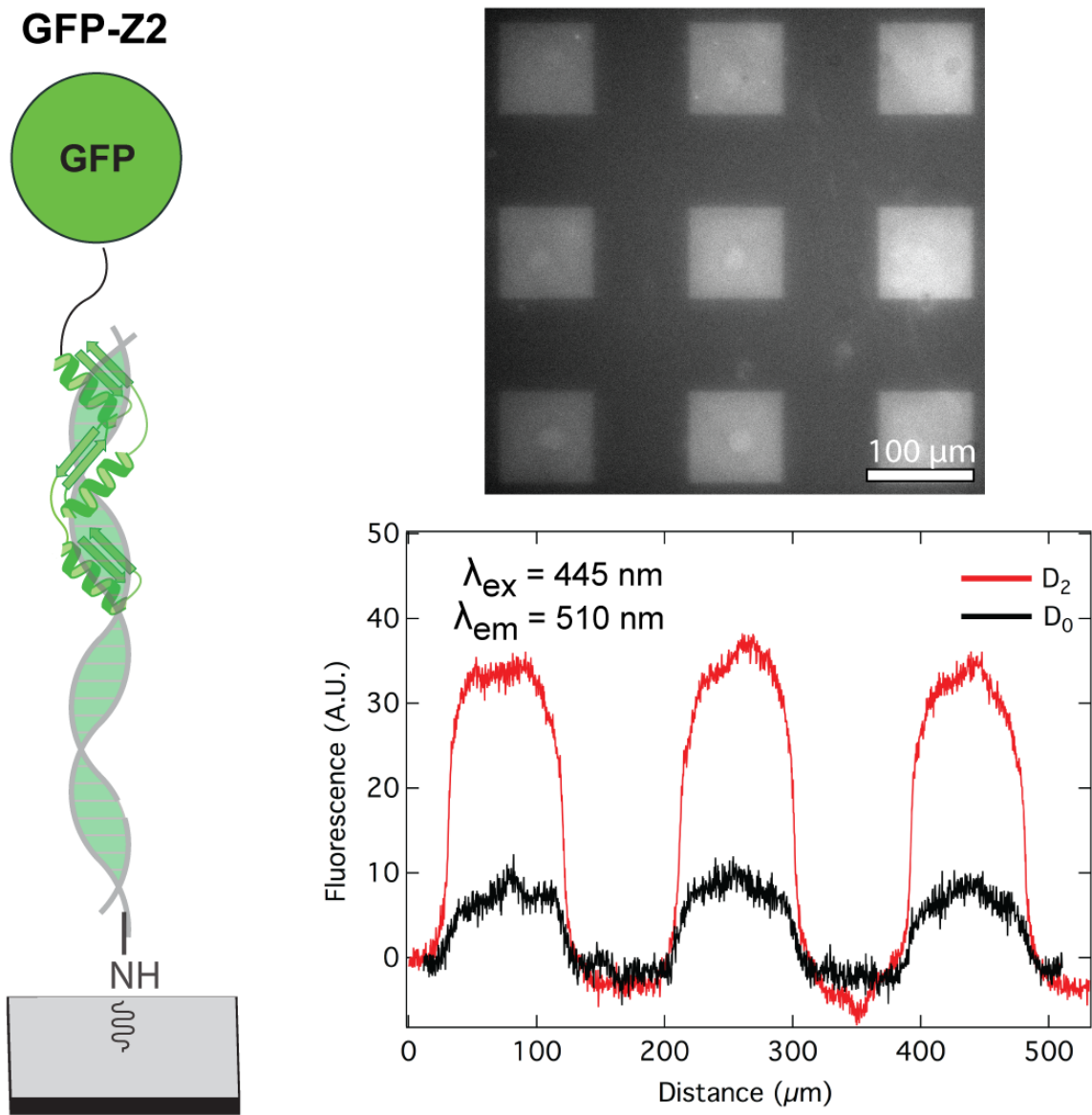
Figure 3A.1 Fluorescence Microscopy of GFP-Z_2 Adsorption to D_2 surface. Fluorescence from adsorption to a D_0 surface was also measured, though the image is not shown. The images were integrated and plotted, showing 4-fold more fluorescence for the D_2 surface over the D_0 surface.
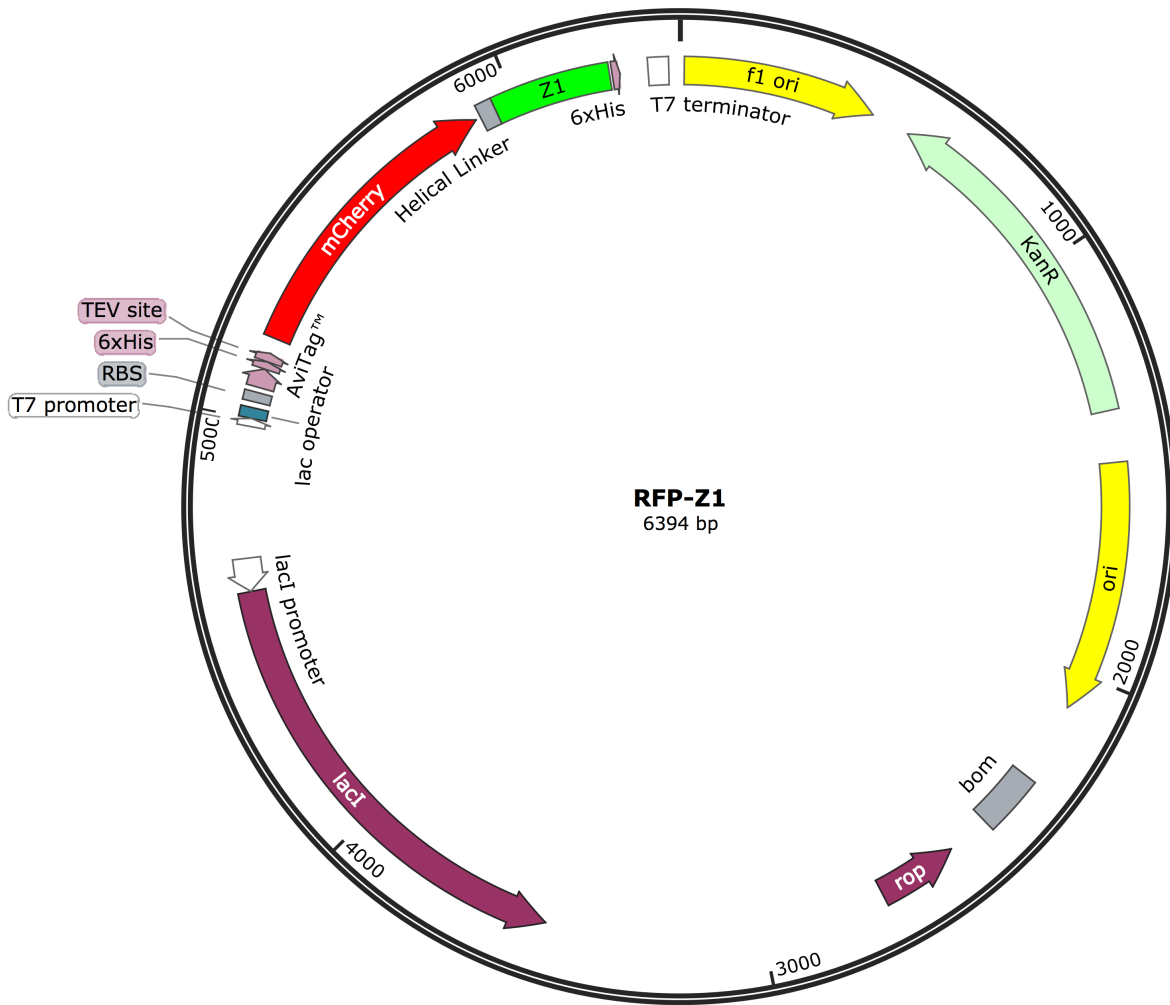
Figure 3A.2 Vector Map of RFP-Z$_1$. This DNA was synthesized by LIC and confirmed by Sanger sequencing. This full vector was used in IVTT experiments without further modification.
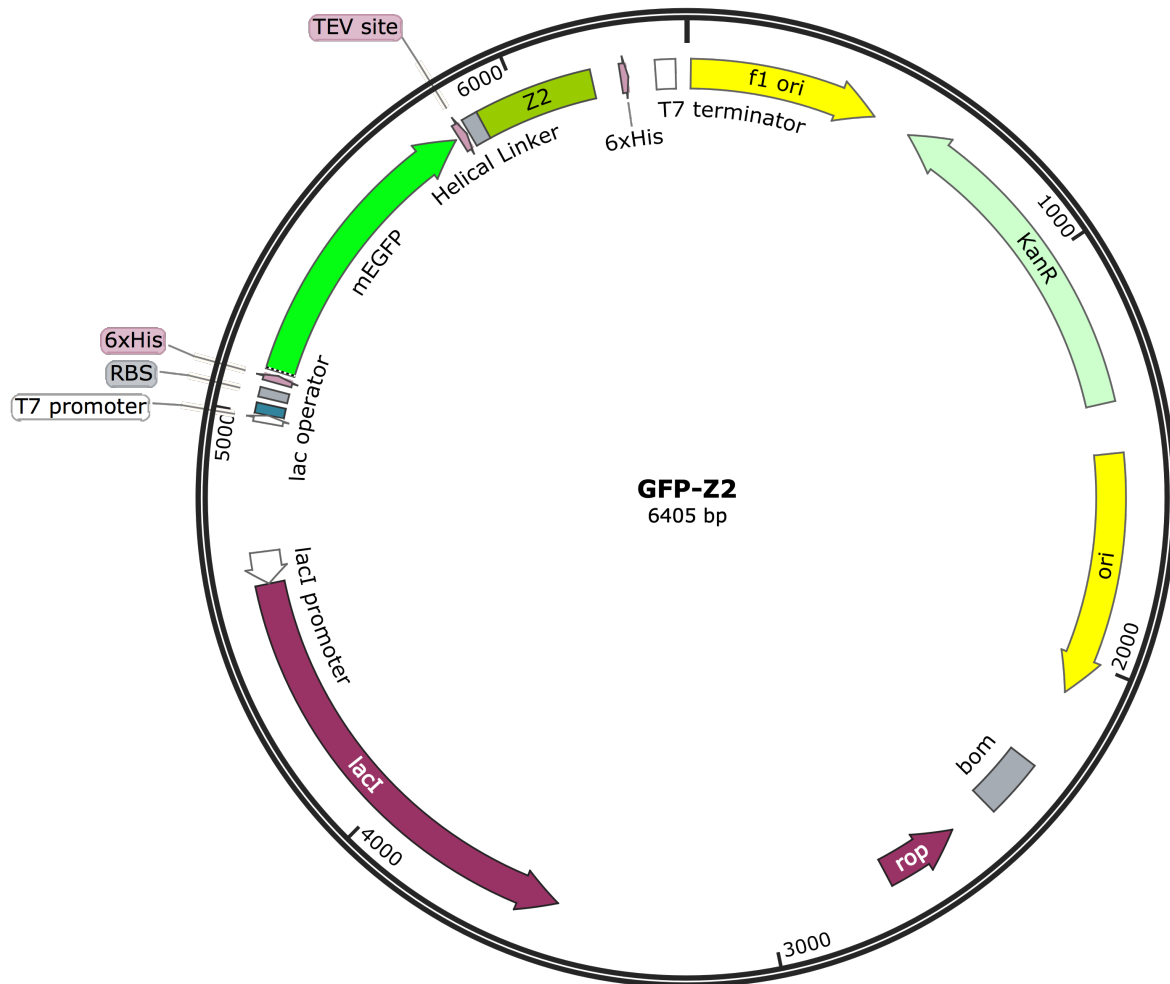
Figure 3A.3 Vector Map of GFP-Z$_2$ This DNA was synthesized by LIC and confirmed by Sanger sequencing. This full vector was used in IVTT experiments without further modification.

Chapter 4

Progress Toward a Templated Biosynthesis Fabrication Method for the Incorporation of Unnatural Amino Acids into Protein Microarrays

4.1 Introduction

4.1.1 Background and Strategy Overview

Proteins containing unnatural amino acids (unnatural proteins) have emerged as useful tools for elucidation of protein function.[1–3] These amino acids offer chemists precise chemical control of a protein beyond the chemistries offered by the 20 canonical amino acids. For example, the incorporation of methylated,[4] phosphorylated,[5,6] and glycosylated amino acids[7] into proteins have allowed researchers to study the effects of site-specific posttranslational modifications. The incorporation of amino acids containing NMR and UV-Vis probes allowed researchers to study protein dynamics.[8,9] Additionally, UV-labile protecting groups,[10] radical initiators,[11] and small molecule fluorophores[12–15] have all been incorporated into proteins as unnatural amino acids (UAAs) to study a variety of functions. Despite the incredible breadth of functionality UAAs provide, they have yet to be incorporated into protein microarray fabrication strategies.

In this chapter, we describe progress toward the fabrication of unnatural protein microarrays suitable for SPRI. Our strategy is outlined in Figure 4.1 and is analogous to the strategy described in Chapter 2.[16] In this strategy, we use amber suppression to site specifically incorporate UAAs into proteins for this microarray. First, we create a microwell array by laser cutting PDMS tape and adhering it to a glass slide. We then add DNA encoding a protein truncated by an amber stop codon along with the IVTT reagents required for amber suppression (Figure 4.1a). Misacylated amber tRNA (tRNA$_{CUA}$) is then added to each well, such that each well contains a tRNA$_{CUA}$ misacylated with a different amino acid (Figure 4.1b). This array is then sealed in a PDMS chamber and incubated at 30°C for protein synthesis. The proteins synthesized in this method differ by a single UAA based upon the misacylated amber tRNA

added (Figure 4.1c). After protein synthesis, the proteins are printed onto a Cu^{II}-NTA chip for

SPRI analysis (Figure 4.1d). This method has the potential to quickly and efficiently screen the

effects of various UAAs in the single site of a protein.
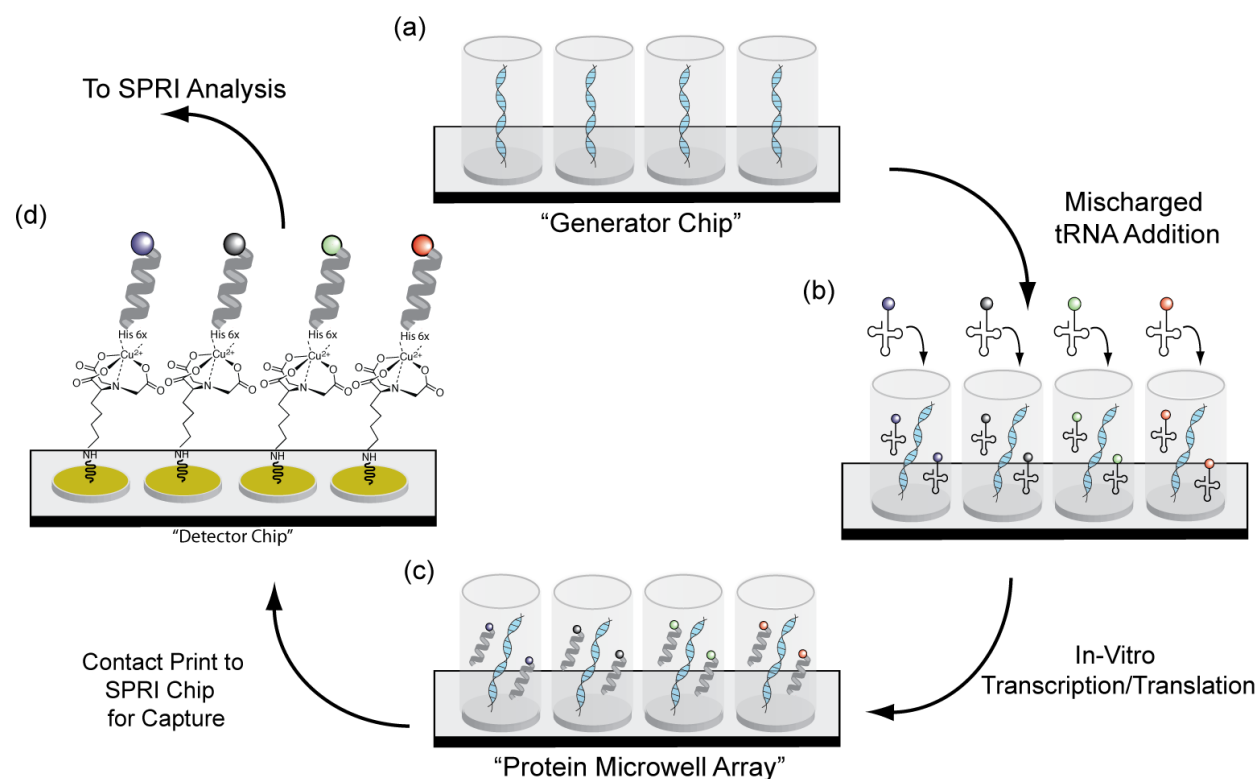
Figure 4.1: Strategy Overview for Unnatural Protein Microarray Fabrication. First a
microwell array is created containing all the components required for amber suppression,
including DNA encoding a protein truncated by an amber stop codon (a). Next, acylated
tRNA$_{CUA}$ is added to each well, such that each tRNA$_{CUA}$ is acylated with a different amino
acid (a). The tRNA$_{CUA}$ added in the previous step dictates the amino acid incorporated into
the proteins in this step. The resulting protein microwell array (c) is then contact printed onto
a functionalized SPRI chip for bioaffinity analysis (d).

4.1.2 Amber Suppression Overview

Amber suppression is one of many methods used to incorporate UAAs into proteins. In

contrast to other popular methods, amber suppression has the advantage of being compatible

with ribosomal biosynthesis, greatly reducing synthesis time and the number of synthetic steps

demanded by other leading unnatural protein synthesis methods, such as solid phase peptide synthesis or native chemical ligation.[17–19] An overview of amber suppression is outlined in Figure 4.2. Classic prokaryotic translation is shown in Figure 4.2a. In protein biosynthesis, a gene is transcribed into messenger RNA (mRNA) and is then translated into proteins via ribosome catalyzed amino acid polymerization. Translation is typically terminated via one of three common stop codons: UAG ("amber"), UAA ("ochre"), or UGA ("opal").[20] Proteins called release factors (RFs) recognize these stop codons and terminate translation upon binding (Figure 4.2a).

In amber suppression strategies for the incorporation of UAAs (Figure 4.2b), artificial tRNA partners for the amber stop codon (tRNA$_{CUA}$) are included in the biosynthesis reaction, giving researchers an additional, orthogonal codon for site-specific UAA incorporation. In the
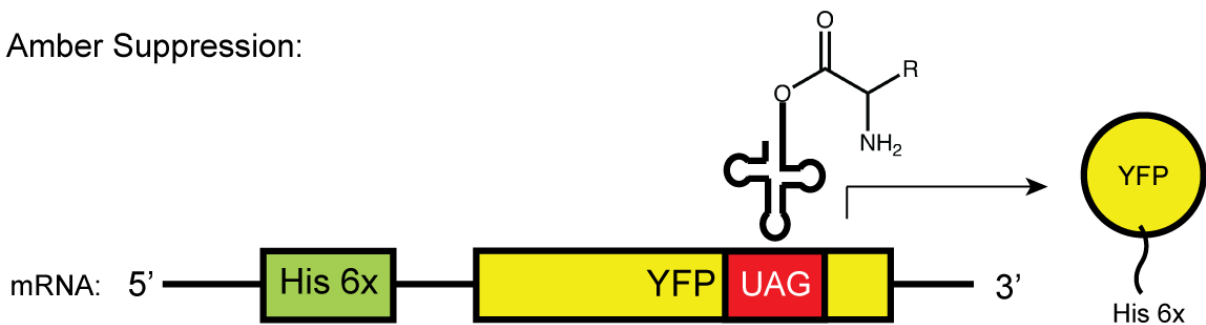
Figure 4.2: Amber Suppression Overview: A basic outline of amber suppression is shown. (a) In canonical biosynthesis, an amber stop codon (UAG) is read by RF1, terminating translation. In this case, the amber codon is in the middle of YFP, resulting in a truncated protein upon termination. In amber suppression (b), an amber tRNA is added to the reaction mixture. In the presence of an amber tRNA, translation continues through the amber stop codon and a full protein is synthesized.
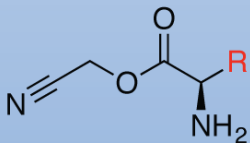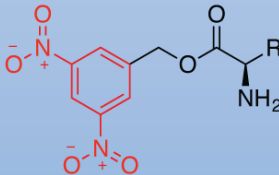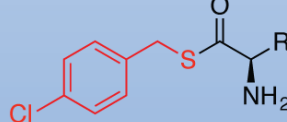
absence of the RF1, the release factor for the amber codon, tRNA$_{CUA}$ reads through the amber stop codon and its amino acid is incorporated. This powerful strategy gives researchers the ability to (i) choose virtually any amino acid, natural or unnatural, for incorporation into proteins and (ii) the ability to choose the location of their chosen amino acid.

Amber suppression is dependent on the misacylation of tRNA$_{CUA}$ with an amino acid. Misacylation of tRNA$_{CUA}$ is commonly achieved enzymatically via aminoacyl tRNA synthetases (aaRSs). These ATP-dependent enzymes acylate the 3'-OH of a tRNA with an amino acid and are specific for a single tRNA/amino acid pair. In order to increase the promiscuity of these enzymes to accept an tRNA$_{CUA}$/UAA pair, researchers have found success introducing mutations into the amino acid binding pockets of the tRNA$_{CUA}$ specific aaRS of *M. jannaschii*.[21] Though this strategy has been fruitful, yielding a variety of tRNA$_{CUA}$/aaRS pairs capable of misacylating many different UAAs, the process to create these pairs is difficult, requiring many rounds of positive and negative selections via *E. coli*.[22] With the goal of creating an unnatural protein microarray fabrication method that is universally accessible, a simpler and easily scalable misacylation method must be considered.

4.1.3 tRNA$_{CUA}^{Asn}$ Misacylation by Flexizyme System

To make amber suppression more accessible, Suga *et. al.* have developed a ribozyme based tRNA acylation system, termed the Flexizyme system. In contrast to aaRS based tRNA charging, Flexizyme charges any tRNA regardless of its anti-codon as long as it is presented with an activated amino acid bearing the correct recognition group (Table 4.1). Each of the 3 classes of Flexizyme listed in Table 4.1 have their niche in functionality; the original flexizyme (Fx)[23] can only acylate amino acids that have aryl R-groups, while dinitro-flexizyme (dFx) can acylate

Table 4.1: Flexizyme Variants and Their Activated Amino Acid Counterparts: Each flexizyme is designed for acylation of specific types of amino acids. These ribozymes also differ in their amino acid binding regions (red).

Flexizyme:	Fx	dFx	eFx
Activated Amino Acid:	R = Aryl	R = Non β-Branched	R = Any

all but β-branched amino acids.[24] Enhanced-flexizyme (eFx) covers the deficiencies of dFx and

is able to acylate β-branched amino acids.[24]

      An outline of the Flexizyme system is shown in Figure 4.3. First, the chosen flexizyme,

the tRNA, the activated amino acid are mixed. The amino acid is present in 50-fold excess over

the two RNAs (Figure 4.3a). When cooled, the ternary complex shown in Figure 4.3b is formed.

The flexizyme and the tRNA anneal via the 3'-CCA of the tRNA and the amino acid binds to the

binding pocket of the flexizyme, positioning the amino acid in close proximity to the 3'-OH of

the tRNA for acylation.[25] After a 12 h incubation period at 4°C, the acylated tRNA is formed

(a)   (b)   (c)
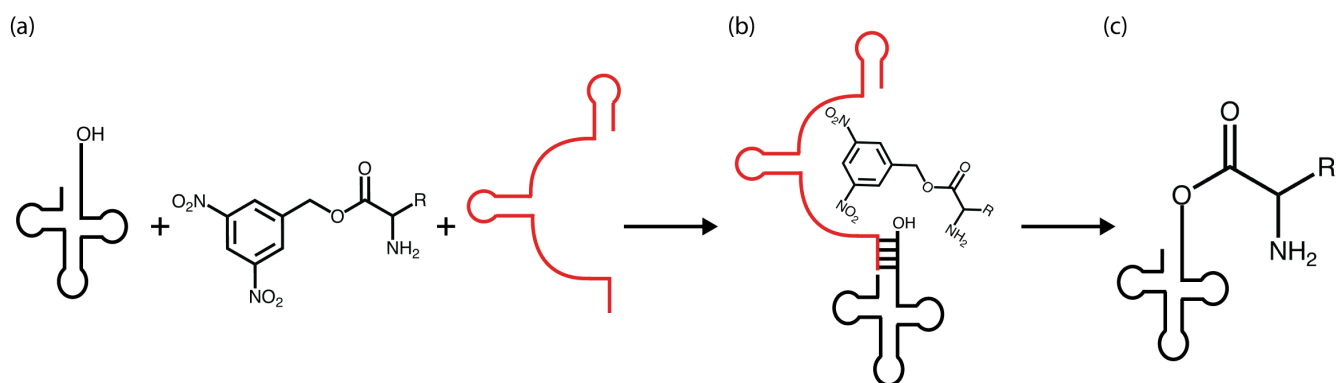
Figure 4.3 Flexizyme Catalyzed Misacylation of tRNA: For this example, misacylation of a tRNA by dFx is shown. (a) An equimolar mixture of tRNA and dFx are mixed followed by the addition of 50 equivalents of activated amino acid. Upon mixing and cooling, the ternary complex (b) is formed, positioning the amino acid for acyl attack by the 3'-OH of the tRNA.

(Figure 4.3c). The tRNAs are then purified by PAGE and used in downstream amber suppression experiments.

This method is highly modular in the types of tRNAs and amino acids that can be accommodated, making this system a suitable candidate for the tRNA misacylation steps required for unnatural protein microarray fabrication.

4.1.4 YFP Recoding by Amber Suppression

As a proof-of-concept, we will first perform amber suppression using canonical amino acids. To do this, we will mutate H77 of the of 10C Q69K variant of yellow fluorescent protein (YFP) into an amber codon (TAG). We will then acylate an amber tRNA ($tRNA_{CUA}^{Asn}$) with histidine via the flexizyme system and perform on-chip IVTT in the same manner as in Chapter 2. Analysis by fluorescence microscopy will be used to estimate suppression efficiency and then the microwell array will be used to contact print the resulting recoded YFP onto a Cu^{II}-NTA functionalized SPRI chip.

4.2 Experimental Considerations

4.2.1 Chemicals and Materials

All chemicals were purchased from Sigma-Aldrich unless otherwise stated. SF-10 glass slides (18 × 18 mm) were purchased from Schott AG. N-succinimidyl-S-acetylthiopropionate (SATP) was purchased from Pierce. Maleimide poly-ethyleneglycol (350 Da) was purchased from NanoCS. Maleimido-C3-nitrilotriacetic acid and 11-mercaptoundecamine (MUAM) were purchased from Dojindo. Polyclonal anti-GFP was purchased from Abcam. YFP filter cubes were purchased from Thor Labs and used for fluorescnece imaging of recoded YFP. All DNAs

were purchased from Integrated DNA Technologies unless otherwise specified. All water used was obtained by a Milli-Q integral water purification system.

4.2.2 RNAs Used In This Study

tRNA$_{CUA}^{Asn}$:[26,27] 5'-GUC CUC UGU AGU UCA GUC GGU AGA ACG GCG GAC UCU AAA UCC GUA UGU CAC UGG UUC GAG UCC AGU CAG AGG CCA CCA-3'

dFx Flexizyme:[24] 5'-GGA UCG AAA GAU UUC CGC AUC CCC GAA AGG GUA CAU GGC GUU AGGU-3'

4.2.3 Synthesis of O-3,5-dinitrobenzyl-L-hisidine for tRNA$_{CUA}^{Asn}$ Misacylation (1)

This procedure was adapted from Murakami *et al.*[24] First, 300 mg (1.18 mmol) of N$_\alpha$-boc-L-histidine was added to 10 mL of dimethylformamide. Then, 164 uL (1.18 mmol) of triethylamine was added to the solution, mixed until homogenous, and was cooled to 0°C. After cooling, 215.6 mg (0.802 mmol) of 3,5-dinitrobenzyl chloride was added and then the solution was allowed to warm to room temperature. The reaction was then heated to 60°C and was stirred overnight. The reaction was judged to be complete by thin layer chromatography after mixing for 12 h. Ethyl acetate (20 mL) was added to the completed reaction and the resulting solution was washed with 5 mL of saturated sodium bicarbonate (3x) followed by 5 mL of water (3x). The organic portion was dried over magnesium sulfate and reduced *in vacuo* yielding a yellow oil. This oil was dissolved in 2 mL of ethyl acetate, then 2 mL (6 mmol) of 4 M HCl in dioxane was added to remove the boc-protecting group from the α-amine. A yellow precipitate formed after mixing for 1 h at room temperature. The precipitated was filtered and washed with diethyl ether (5 mL x 3) yielding **(1)** in 86% yield.

^{1}H NMR (500 MHz, d_6-DMSO): δ 7.97 (1H, J=1.5, d), 7.76 (1H, J=2.5 t), 7.67 (2H, J=2.5 d), 6.46 (1H, br), 4.43 (2H, $\Delta\delta_{AB}$=0.35, J=18, ABq), 3.57 (1H, J=7 t), 2.35 (2H, J=7 d). ^{13}C NMR (500 MHz, d_6-DMSO): δ 167.73, 147.98, 139.28, 133.88, 128.69, 126.66, 118.43, 118.07, 66.34, 65.29, 51.04, 25.04. HRMS (ESI/Q-TOF) m/z: $[M + H]^+$ 336.0055; $[M + Na]^+$ 358.9800.

4.2.4 Mutagenesis of YFP from GFP DNA

DNA encoding the 10C Q69K variant of YFP[28] was prepared from DNA encoding wild-type green fluorescent protein (wtGFP) by site directed mutagenesis. The wtGFP DNA was obtained from the 5PRIME RTS protein synthesis system (Promega). This 10C Q69K YFP variant contains the following mutations: S65G, V68L, Q69K, S72A, and T203Y. Site directed mutagenesis was performed three times to obtain this variant. The first round of mutagenesis introduced the S65G and V68L mutations, while the second round introduced the Q69K and S72A mutations. The third and final round of mutagenesis introduced the T203Y mutation. After each round of mutagenesis, the resulting DNA was purified, sequenced, and used in the next round of mutagenesis.

Mutagenesis was performed by PCR, using primers that contained the desired sequence changes. For round 1, the following primer and its complement were used (this type of mutagenesis the forward and reverse primers are complements of each other as opposed to traditional PCR): 5'-ACA CTT GTC ACT ACT TTC GGT TAT GGT CTT CAA TGC TTT TCA AGA-3'. The following primers and their complements were used for round 2: 5'-GGT TAT GGT CTT AAA TGC TTT GCA AGA TAC CCG GAT CAT ATG AAA-3', and for round 3: 5'-CCA GAC AAC CAT TAC CTG TCC TAC CAA TCT GCC CTT TCG AAA GAT-3'. DNA changes are denoted in red.

The following PCR reaction was used for each round of mutagenesis: 0.5 µL of 20 µM of both reverse and forward primer, 1 µL of 100 ng/µL dsDNA, 10 µL of 2x iProof High Fidelity PCR Master Mix (BioRad), and 7 µL of water were added to a PCR tube. PCR was run for 20 cycles. The mixture was then treated with 1 µL of DPN-I (NEB) and incubated at 37°C for 1 h to selectively digest the template DNA. The mixture was then analyzed by 2% agarose gel electrophoresis and visualized by ethidium bromide stain. After confirmation of the correct PCR product, the product was used directly for transformation into competent *E. coli.* The *E. coli* was then plated onto LB agar containing 40 µg/mL kanamycin and was incubated overnight at 37°C. Colonies from this plate were then used to inoculate LB broth containing 40 µg/mL kanamycin and were allowed to grow overnight at 37°C with shaking. DNA from these overnight colonies were extracted using a QIAprep Plasmid Miniprep Kit (Qiagen), sequenced, and used in downstream mutagenesis or IVTT experiments.

4.2.5 Preparation of 10C Q69K YFP (H77TAG)

An amber codon was introduced into position 77 of the 10C Q69K YFP variant using the same general PCR site directed mutagenesis strategy described in the previous section. The following primer and its complement were used: 5'- GCA AGA TAC CCG GAT TAG ATG AAA CGG CAT GAC TTT TTC AAG AGT -3'. DNA changes are denoted in red.

4.2.6 Flexizyme Reaction for misacylation of tRNA$_{CUA}^{Asn}$

This reaction was performed as described by Murakami *et al.*[24] First, 4 µL of 100 µM tRNA$_{CUA}^{Asn}$ was added to 2 µL of 1 M HEPES (pH 7.5) in a PCR tube. The solution was heated to 95°C and was allowed to incubate for 5 min. The reaction was cooled to 25°C and was allowed

78

to rest for 5 min. These heating and cooling steps were performed to ensure correct tRNA secondary structure. Then, 4 μL of 3 M aqueous $MgCl_2$ and 4 μL of 100 μM dFx were added to the resulting mixture and mixed by vortex. This solution was incubated at 25°C for 5 min. Then, 2 μL of DMSO and 2 μL of 50 mM 3,5-dinitrobenzyl ester-L-histidine were then added, mixed by vortex, and incubated at 4°C for 14 h. After this incubation period, a white precipitate formed at the bottom of the PCR tube. 45 μL of 600 mM NaOAc (pH 5) was added to stop the reaction and the RNAs were precipitated by classical ethanol precipitation techniques. The precipitated RNAs were reconstituted in 5 μL of water to an estimated total $tRNA_{CUA}^{Asn}$ concentration of 80 μM as measured by Nanodrop. This solution was used in downstream IVTT experiments.

4.2.8 PURE System IVTT for Amber Suppression

Amber suppression was performed using the PURExpress Δ RF123 kit from NEB. The following components were assembled on ice: 5 μL of solution A, 3.75 μL of solution B, 0.25 μL of RF2, 0.25 μL of RF3, 2 μL of 300 ng/μL YFP amber DNA, 0.5 uL of glycerol, and 1.25 μL of 80 uM total $tRNA_{CUA}^{Asn}$ from Section 4.3.5. In experiments which specific components were omitted, the volume was replaced with water. The resulting solution was gently mixed and added to the microwell array. The microwell array was then incubated under a PDMS chamber at 30°C for 6 h followed by 4°C overnight in the same manner as in Chapter 2.

4.2.9 Microwell Array Fabrication

Microwell array fabrication was performed as described in Section 2.2.2.

4.2.10 Fluorescence Microscopy

Fluorescence microscopy was performed as described in section 2.2.5

4.2.11 SPRI Experiments

SPRI Experiments were performed as described in section 2.2.9

4.3 Results and Discussion

4.3.1 Design of amber EYFP

In order to evaluate the potential of on-chip amber suppression as a suitable strategy for unnatural protein microarray fabrication, we first developed a system to readily estimate amber suppression efficiency on-chip while also assessing the compatibility of the resulting proteins with SPRI. Fluorescent proteins are perfectly suited for this type of system because their fluorescence is reliant on full-length biosynthesis. This property allows us to introduce an amber codon such that successful amber suppression is required to observe fluorescence. Further, fluorescence is a concentration dependent phenomenon, allowing us to estimate amber suppression efficiency via fluorescence.

The 10C Q69K variant of YFP was chosen for these amber suppression experiments because of its well-characterized fluorescence properties and our familiarity with the protein in SPRI studies. An amber codon was inserted in place of histidine 77 by site directed mutagenesis. Histidine 77 was chosen for two reasons: first, position 77 is in the middle of YFP, so in non-suppression conditions, translation results in a truncated, non-fluorescent protein (Figure 4.2b). Second, position 77 is solvent exposed and amber suppression has been shown to be more efficient at solvent exposed positions that have little secondary structure.[3]

4.3.2 Microwell Biosynthesis of Recoded YFP

To perform amber suppression in a microwell array, we preferred to use the protein synthesis using recombinant elements (PURE) system.[29] These types of cell-free expression systems give researchers the flexibility to include or omit any components of the IVTT reaction. This is particularly advantageous for amber suppression, because this system allows us to omit the main competitor for amber suppression, release factor 1 (RF1).

Purified IVTT solutions were prepared without RF1 and these solutions were added to a microwell array prepared in the same manner as in Chapter 2. Then, $tRNA_{CUA}^{Asn}$, misacylated with histidine via the Flexizyme system, was added to these IVTT solutions and the microwell array was sealed and incubated at 30°C for 30 minutes. The PDMS chamber was removed and the array was placed in a humidity chamber. The array and chamber were incubated at 4°C for at least 2 hours to allow for protein folding. The microwell array was then analyzed by fluorescence microscopy.

Fluorescence images of the microwell arrays are shown in Figure 4.4. Four different reactions were included in the microwell array. The first column (1) of the array contains YFP synthesized by sense codon biosynthesis and is used as a positive control for YFP produced by PURE-IVTT. The second column (2) of the array contains YFP produced by amber suppression. Column three (3) of the microwell array contains reactions in which activated histidine **(1)** is omitted from the misacylation reaction, while column four (4) contains reactions in which dFx, $tRNA_{CUA}^{Asn}$, and **(1)** are all omitted. Columns three and four are used as negative controls. Based on the integrated fluorescence data, we estimate an amber suppression efficiency of 64% (Figure 4.4 column 2) compared to sense codon translation of YFP (Figure 4.4 column 1). This

	1	2	3	4
Amber tRNA	NA	+	+	−
Amber dsDNA	NA	+	+	+
eFx	NA	+	+	−
DBE-His	NA	+	−	−
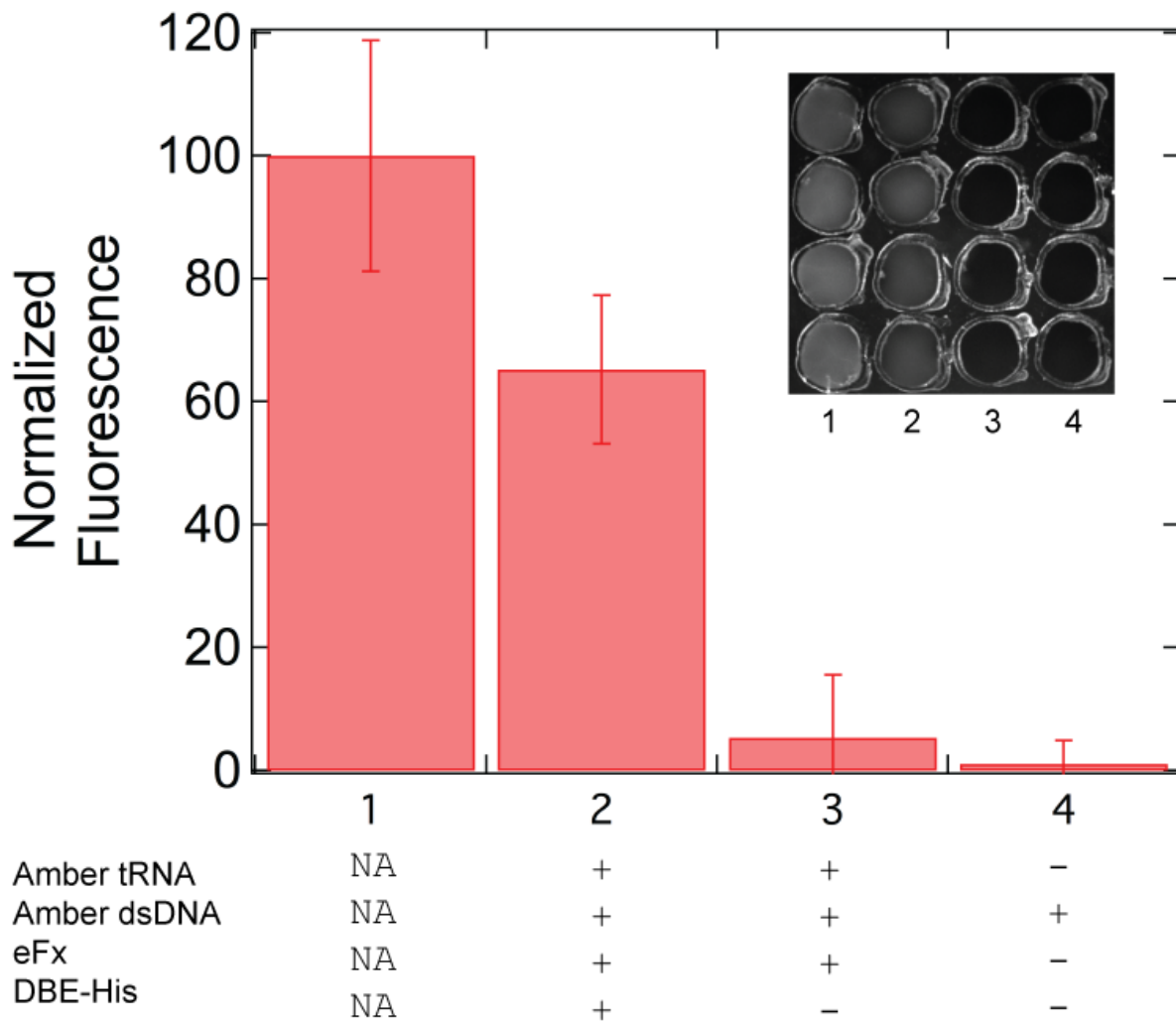
Figure 4.4 Fluorescence Microscopy of On Chip Amber Suppression of YFP. Amber suppression of YFP was performed on chip and the resulting fluorescence from synthesized YFP was measured. In column 1, YFP produced by canonical biosynthesis was produced for a positive control. In column 2, YFP produced by amber suppression is shown. Column 3 contains reactions in which DBE-His was omitted from the flexizyme reaction, while column 4 contains reactions that contain only DNA encoding amber YFP.

efficiency is comparable to other amber suppression studies.[30] Further, these data show that all components of the flexizyme misacylation reaction are required for successful amber suppression. In wells in which activated histidine **(1)** was omitted from the misacylation reaction, we observe an acylation efficiency of only 5%, while in wells that omit all reagents required for misacylation, the efficiency decreases to 1%. We attribute these small amounts of amber suppression to read-through by endogenous tRNAs, a phenomenon which has been observed in other amber suppression studies.[31]

To measure the concentration of the proteins created by this method, IVTT solutions were removed from their microwells and fluorescence was measured against a YFP standard of known concentration. Sense codon translation of YFP in this microwell array format produced approximately 2.4 picograms of protein, translating to a 4.8 μM protein solution produced in wells. YFP produced by amber suppression yielded approximately 1.4 picograms of protein, translating to a 2.8 μM protein solution. These values translate into an amber suppression efficiency of 58%, which is in agreement to the efficiencies calculated by the integrated fluorescence images. The slight discrepancy of 6% efficiency between the two measurements are likely due to batch-to-batch variation.

These experiments show that amber suppression is possible in a microwell format with efficiencies that are comparable to other *in vitro* amber suppression methodologies. Having shown that we can perform amber suppression on-chip, we need to confirm that the proteins produced using this methodology can be used in downstream SPRI experiments for the detection of protein/protein interactions.

4.3.3 Surface Plasmon Resonance Imaging of Recoded YFP

Using the recoded YFP microwell arrays described in the previous section, we used the contact printing methodology described in Chapter 2 to transfer these proteins to a Cu^{II}-NTA functionalized SPRI chip. This resulting protein microarray was then used to detect polyclonal anti-GFP. A 20 nM solution of polyclonal anti-GFP was introduced to the printed array and as shown in Figure 4.5, elements printed with YFP synthesized by sense codon IVTT show a Δ%R of 0.90 ± 0.13%. Elements printed with recoded YFP synthesized by amber suppression result in
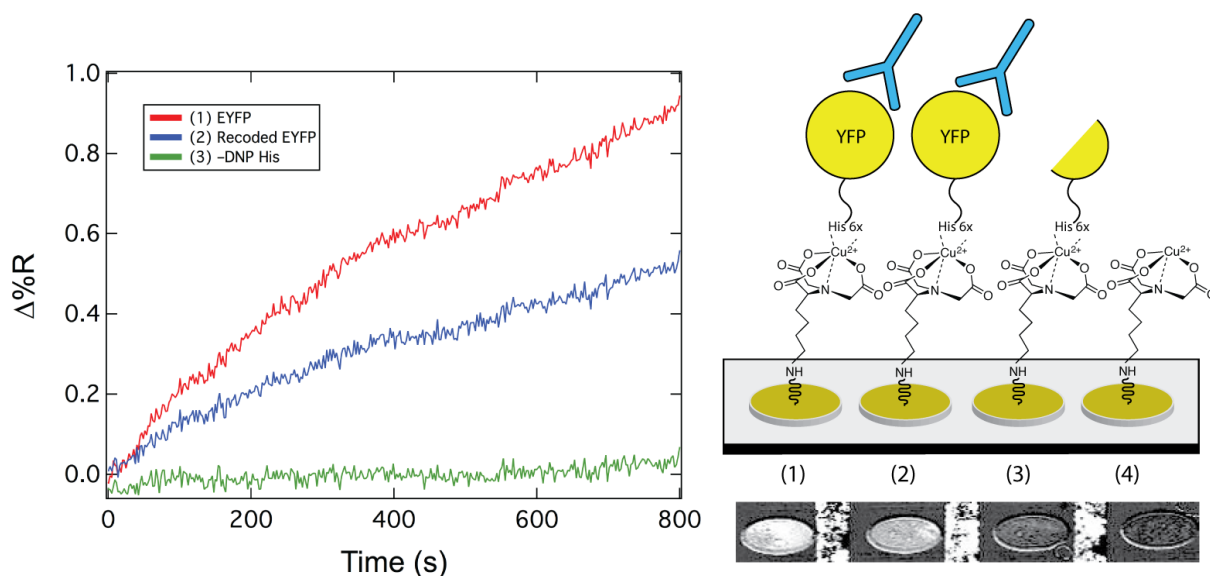
Figure 4.5 SPRI of Polyclonal anti-GFP Created by Amber Suppression: YFP created by amber suppression was synthesized in a microwell array and contact printed onto an NTA-functionalized SPRI chip. Polyclonal anti-GFP was introduced to the resulting protein microarray. SPRI kinetics measurements are shown (left) as well is difference images (bottom right). (1) YFP created by sense codon biosynthesis. (2) Recoded YFP created by amber suppression. (3) Activated histidine omitted from flexizyme acylation. (4) All flexizyme components omitted.

a Δ%R of 0.56 ± 0.02%, while elements printed with truncated YFP showed a Δ%R of 0.04% ± 0.02%. PURE-IVTT alone was used as a blank. The anti-GFP adsorption signal obtained from YFP synthesized by amber suppression is 58% of the signal obtained from adsorption to YFP synthesized by sense codon translation. This difference is consistent with the amber suppression

efficiency observed in the previous section. The signal obtained from anti-GFP adsorption to truncated YFP is 3% of the signal of YFP synthesized by sense codon translation. This value is also consistent with the amber suppression efficiency values obtained from the previous section

The way in which these SPR signals scale with concentration from the solutions they are printed from is due to the relatively low concentrations of proteins produced by the PURE system. In our previous microwell study, proteins were being synthesized at much higher concentrations (40 picograms or 80 μM). These concentrations ensured the saturation of His-tagged proteins on the surface because concentrations were high above the K_d of the His-tag/Cu^{II}-NTA interaction (1-7 μM as measured by SPR).[32] Because concentrations in these amber suppression experiments are close to the K_d of the His-tag/Cu^{II}-NTA interaction, we expect adsorption to scale with concentration as governed by equilibrium. Therefore, we are not saturating the SPRI elements with proteins and the SPRI signal obtained from polyclonal anti-GFP adsorption should scale with protein concentration, which is what we observe in our experiments.

These SPRI experiments clearly show that proteins created by amber suppression can be printed onto a functionalized SPRI chip and used for the detection of antibody adsorption. However, these experiments also expose a limitation in relatively low synthesis yields compared to our previous microwell array studies. This issue will only be amplified as we attempt to incorporate more complex unnatural amino acids into more complicated proteins, so it is imperative that the yields of these reactions be increased.

4.4 Conclusions

In this chapter, we show progress toward an unnatural protein microarray fabrication method for SPRI. As a proof of concept, we used an amber suppression strategy to synthesize recoded YFP in a microwell array and observed suppression efficiencies that are comparable to other reported *in vitro* methods. This microwell array can also be printed onto a Cu^{II}-NTA functionalized SPRI chip for protein/protein analysis.

The work presented in this chapter is a strong first step towards our ultimate goal of an unnatural protein microarray fabrication method. In order for this goal to be realized, it is imperative that we explore the scope of UAAs that can be incorporated via this method. Next, yields for on chip synthesis must be increased in order to eliminate the effect of amber suppression efficiency on adsorption to the SPRI surface. It is also important this microarray finds functional use for the screening of natural and unnatural amino acids in a single site of a protein. This screening should not be limited to only protein/protein interactions, but also to enzyme function.

4.5 Acknowledgments

4.6 References

(1)   Dougherty, D. A. Unnatural Amino Acids as Probes of Protein Structure and Function. *Curr. Opin. Chem. Biol.* **2000**, *4* (6), 645–652.

(2)   Sletten, E. M.; Bertozzi, C. R. Bioorthogonal Chemistry: Fishing for Selectivity in a Sea of Functionality. *Angew. Chem. Int. Ed.* **2009**, *48* (38), 6974–6998.

(3)   Liu, C. C.; Schultz, P. G. Adding New Chemistries to the Genetic Code. *Annu. Rev. Biochem.* **2010**, *79* (1), 413–444.

(4)   Nguyen, D. P.; Garcia Alai, M. M.; Kapadnis, P. B.; Neumann, H.; Chin, J. W. Genetically Encoding Nϵ-Methyl-L-Lysine in Recombinant Histones. *J. Am. Chem. Soc.* **2009**, *131* (40), 14194–14195.

(5)   Park, K. D.; Liu, R.; Kohn, H. Useful Tools for Biomolecule Isolation, Detection, and Identification: Acylhydrazone-Based Cleavable Linkers. *Chem. Biol.* **2009**, *16* (7), 763–772.

(6)   Steinfeld, J. B.; Aerni, H. R.; Rogulina, S.; Liu, Y.; Rinehart, J. Expanded Cellular Amino Acid Pools Containing Phosphoserine, Phosphothreonine, and Phosphotyrosine. *ACS Chem. Biol.* **2014**, *9* (5), 1104–1112.

(7)   Fahmi, N. E.; Dedkova, L.; Wang, B.; Golovine, S.; Hecht, S. M. Site-Specific Incorporation of Glycosylated Serine and Tyrosine Derivatives into Proteins. *J. Am. Chem. Soc.* **2007**, *129* (12), 3586–3597.

(8)   Jackson, J. C.; Hammill, J. T.; Mehl, R. A. Site-Specific Incorporation of a 19F-Amino Acid into Proteins as an NMR Probe for Characterizing Protein Structure and Reactivity. *J. Am. Chem. Soc.* **2007**, *129* (5), 1160–1166.

(9)   Schultz, K. C.; Supekova, L.; Ryu, Y.; Xie, J.; Perera, R.; Schultz, P. G. A Genetically

        Encoded Infrared Probe. *J. Am. Chem. Soc.* **2006**, *128* (43), 13984–13985.

(10)   Wu, N.; Deiters, A.; Cropp, T. A.; King, D.; Schultz, P. G. A Genetically Encoded

        Photocaged Amino Acid. *J. Am. Chem. Soc.* **2004**, *126* (44), 14306–14307.

(11)   Chou, C.; Uprety, R.; Davis, L.; W. Chin, J.; Deiters, A. Genetically Encoding an

        Aliphatic Diazirine for Protein Photocrosslinking. *Chem. Sci.* **2011**, *2* (3), 480–483.

(12)   Summerer, D.; Chen, S.; Wu, N.; Deiters, A.; Chin, J. W.; Schultz, P. G. A Genetically

        Encoded Fluorescent Amino Acid. *Proc. Natl. Acad. Sci.* **2006**, *103* (26), 9785–9789.

(13)   Wang, J.; Xie, J.; Schultz, P. G. A Genetically Encoded Fluorescent Amino Acid. *J. Am.

        Chem. Soc.* **2006**, *128* (27), 8738–8739.

(14)   Louie, G. V.; Takimoto, J. K.; Noel, J. P.; Lee, K.-F.; Wang, L.; Slesinger, P. A.; Baiga, T.

        J.; Wang, W. Genetically Encoding Unnatural Amino Acids for Cellular and Neuronal

        Studies. *Nat. Neurosci.* **2007**, *10* (8), 1063.

(15)   Steward, L. E.; Collins, C. S.; Gilmore, M. A.; Carlson, J. E.; Ross, J. B. A.; Chamberlin,

        A. R. In Vitro Site-Specific Incorporation of Fluorescent Probes into β-Galactosidase. *J.

        Am. Chem. Soc.* **1997**, *119* (1), 6–11.

(16)   Manuel, G.; Lupták, A.; Corn, R. M. A Microwell–Printing Fabrication Strategy for the

        On-Chip Templated Biosynthesis of Protein Microarrays for Surface Plasmon Resonance

        Imaging. *J. Phys. Chem. C* **2016**.

(17)   Kent, S. B. H. Chemical Synthesis of Peptides and Proteins. *Annu. Rev. Biochem.* **1988**, *57*

        (1), 957–989.

(18)   Dawson, P. E.; Muir, T. W.; Clark-Lewis, I.; Kent, S. B. Synthesis of Proteins by Native

        Chemical Ligation. *Science* **1994**, *266* (5186), 776–779.

(19)   Muir, T. W. Semisynthesis of Proteins by Expressed Protein Ligation. *Annu. Rev. Biochem.* **2003**, *72* (1), 249–289.

(20)   Scolnick, E.; Tompkins, R.; Caskey, T.; Nirenberg, M. Release Factors Differing in Specificity for Terminator Codons. *Proc. Natl. Acad. Sci. U. S. A.* **1968**, *61* (2), 768–774.

(21)   Wang, L.; Magliery, T. J.; Liu, D. R.; Schultz, P. G. A New Functional Suppressor tRNA/Aminoacyl−tRNA Synthetase Pair for the in Vivo Incorporation of Unnatural Amino Acids into Proteins. *J. Am. Chem. Soc.* **2000**, *122* (20), 5010–5011.

(22)   Wang, L.; Schultz, P. G. A General Approach for the Generation of Orthogonal tRNAs. *Chem. Biol.* **2001**, *8* (9), 883–890.

(23)   Murakami, H.; Saito, H.; Suga, H. A Versatile tRNA Aminoacylation Catalyst Based on RNA. *Chem. Biol.* **2003**, *10* (7), 655–662.

(24)   Murakami, H.; Ohta, A.; Ashigai, H.; Suga, H. A Highly Flexible tRNA Acylation Method for Non-Natural Polypeptide Synthesis. *Nat. Methods* **2006**, *3* (5), 357–359.

(25)   Xiao, H.; Murakami, H.; Suga, H.; Ferré-D'Amaré, A. R. Structural Basis of Specific tRNA Aminoacylation by a Small in Vitro Selected Ribozyme. *Nature* **2008**, *454* (7202), 358–361.

(26)   Cload, S. T.; Liu, D. R.; Froland, W. A.; Schultz, P. G. Development of Improved tRNAs for in Vitro Biosynthesis of Proteins Containing Unnatural Amino Acids. *Chem. Biol.* **1996**, *3* (12), 1033–1038.

(27)   Murakami, H.; Kourouklis, D.; Suga, H. Using a Solid-Phase Ribozyme Aminoacylation System to Reprogram the Genetic Code. *Chem. Biol.* **2003**, *10* (11), 1077–1084.

(28)   Griesbeck, O.; Baird, G. S.; Campbell, R. E.; Zacharias, D. A.; Tsien, R. Y. Reducing the Environmental Sensitivity of Yellow Fluorescent Protein MECHANISM AND APPLICATIONS. *J. Biol. Chem.* **2001**, *276* (31), 29188–29194.

(29)   Kuruma, Y.; Ueda, T. The PURE System for the Cell-Free Synthesis of Membrane Proteins. *Nat. Protoc.* **2015**, *10* (9), 1328.

(30)   Wang, Q.; Parrish, A. R.; Wang, L. Expanding the Genetic Code for Biological Studies. *Chem. Biol.* **2009**, *16* (3), 323–336.

(31)   Chin, J. W. Expanding and Reprogramming the Genetic Code. *Nature* **2017**, *550* (7674), 53.

(32)   Maalouli, N.; Gouget-Laemmel, A. C.; Pinchemel, B.; Bouazaoui, M.; Chazalviel, J.-N.; Ozanam, F.; Yang, Y.; Burkhard, P.; Boukherroub, R.; Szunerits, S. Development of a Metal-Chelated Plasmonic Interface for the Linking of His-Peptides with a Droplet-Based Surface Plasmon Resonance Read-Off Scheme. *Langmuir* **2011**, *27* (9), 5498–5505.